

Review

The Golden Liposomes: Preparation and Biomedical Applications of Gold-Liposome Nanocomposites

Sourour Idoudi, Roua Ismail , Ousama Rachid , Abdelbary Elhissi and Alaaldin M. Alkilany *

College of Pharmacy, QU Health, Qatar University, Doha 2713, Qatar; si1602796@qu.edu.qa (S.I.); ri1703040@student.qu.edu.qa (R.I.); orachid@qu.edu.qa (O.R.); aelhissi@qu.edu.qa (A.E.)

* Correspondence: alkilany@qu.edu.qa

Abstract: Gold nanoparticles (AuNP) have received a growing attention due to their fascinating physicochemical properties and promising range of biomedical applications including sensing, diagnosis and cancer photothermal ablation. AuNP enjoy brilliant optical properties and ability to convert light into local heat and function as a “nanoheaters” to fight cancer. However, AuNP are poor drug delivery systems as they do not have reservoirs or matrices to achieve an acceptable drug loading efficiency. On the other end, liposome-based nanocarriers do not exhibit such optical properties but are excellent platform for drug loading and they have been proven clinically with a true presence in the market since the FDA approved Doxil[®] in 1995. Combining the brilliant optical and photothermal properties of AuNP with the excellent drug loading capability of liposome should yield nanocomposites that enjoy the features of both modalities and enable the development of novel and smart drug delivery systems. Therefore, this review discusses the up-to date research on the AuNP-liposome nanocomposites and the current available approaches and protocols for their preparation and characterization. Finally, the biomedical applications of AuNP-liposome nanocomposites and proposed future directions in this field are discussed.

Keywords: gold; nanoparticles; plasmonic; liposomes; lipid; composites; encapsulation; drug delivery; cancer



Citation: Idoudi, S.; Ismail, R.; Rachid, O.; Elhissi, A.; Alkilany, A.M. The Golden Liposomes: Preparation and Biomedical Applications of Gold-Liposome Nanocomposites. *J. Nanotheranostics* **2023**, *4*, 201–227. <https://doi.org/10.3390/jnt4030010>

Academic Editor: Seyed Moein Moghimi

Received: 12 May 2023

Revised: 22 June 2023

Accepted: 23 June 2023

Published: 25 June 2023



Copyright: © 2023 by the authors. Licensee MDPI, Basel, Switzerland. This article is an open access article distributed under the terms and conditions of the Creative Commons Attribution (CC BY) license (<https://creativecommons.org/licenses/by/4.0/>).

1. Introduction

Nanotechnology has gained a significant interest with broad potential applications in various fields including environment, energy, engineering, and nanomedicine [1–5]. The principal justification of this interest is the unique physicochemical and biological properties of the nanomaterials, which is substantially different at the nanoscale compared to the bulk counterparts [6,7]. Despite the availability of a rich library of nanoparticles from various materials with various shapes, sizes and surface chemistries, no “ideal” platform exists. With this considered, scientists started exploring hybrid systems that combine two or more nanoparticles in an attempt to utilize the best of each component [8].

Gold nanoparticles (AuNP) have received a growing attention due to their brilliant optical properties and wide applications. Under the umbrella of nanomedicine, AuNP have been explored and used for chemical sensing, biomedical diagnosis, drug delivery and targeting, and many other pharmaceutical and biomedical applications [9–12]. This is due to the unique physicochemical, electrical and optical properties of AuNP including their extraordinary capability to absorb/scatter light in the visible-near infra-red (Vis-NIR) region of the spectrum with very large optical extinction coefficients [2,13,14]. Moreover, AuNP convert efficiently absorbed optical energy into local heat, which can be employed to ablate nearby cancer cells or pathogenic organisms [2]. Ease of tunable synthesis and accessible chemistries for surface modifications are additional advantages [15,16]. Furthermore, AuNP possess excellent chemical stability, biocompatibility, and ability to be quantified and visualized in complex biological matrices with sensitivity in vitro and in vivo [2,17,18].

Collectively, the potential properties of AuNP could be applied to develop further targeted and effective systems for future biomedical applications.

A tremendous amount of work has been carried out so far to master the synthesis of AuNP with tunable size, shape and surface chemistry to explore their biomedical applications. Excellent reviews on the synthesis and biomedical applications are available [2,19–23]. Another important direction is the utilization of AuNP in the preparation of novel AuNP-containing composites, in which AuNP could be added to lipidic, polymeric, protein-based or inorganic materials to create a hybrid system that possess mixed functionalities [8,24]. Usually, these nanocomposites hold innovative physicochemical properties to offer new types of applications [8]. In the recent years, several AuNP-based nanocomposites have been prepared including AuNP–carbon nanotubes nanocomposites [25,26], AuNP-polymer nanocomposites [27,28], AuNP-graphene nanocomposites [29], AuNP-metal oxide nanocomposites [30], AuNP-protein nanocomposites [31,32] and AuNP-liposome nanocomposites [33,34]. In previous contributions, we described the facile preparation of AuNP-polymeric nanocomposites and the complete encapsulation of AuNP into PLGA nanocarriers [35,36]. In the current review contribution, we focus on AuNP-liposome nanocomposites. According to Scopus database, searching for review contributions on AuNP-liposome nanocomposites resulted only in two review papers and one book chapter with various focus (Used key words: TITLE (gold AND nano* AND liposome*); search conducted on April 22, 2023) [37–39]. Therefore, this review aims to describe AuNP-liposome nanocomposites with the following objectives:

1. Discuss the outstanding properties of AuNP (the guest) and liposomes (the host) to justify the preparation of AuNP-liposome nanocomposite;
2. Discuss and illustrate various chemistries to prepare AuNP-liposome nanocomposites and analytical tools to confirm and describe the prepared nanocomposites;
3. Highlight and discuss the reported biomedical applications of AuNP-liposome nanocomposites and future directions.

2. Gold Nanoparticles: The Guest

Gold is a Nobel metal with outstanding optical properties at the nanoscale. Michael Faraday's gold colloid (1856) is considered the first preparation of AuNP which is currently on display in Faraday Museum (The Royal Institution, London, UK) [40]. After a century and a half, chemists and physicists developed tremendous wealth of knowledge on the synthesis of much more sophisticated gold nanostructures and fundamentals to understand their optical and photothermal properties [2,19–23].

The optical properties of AuNP arise from the exceptional interaction between photons and electrons of gold at the nanoscale. In more details, the incident photons excite electrons in the conduction band of AuNP resulting in collective oscillation of these electrons to match the wavelength of the incident photons and then the resonating oscillation results in optical extinction (the sum of both optical absorption and scattering). This phenomenon is termed as the Localized surface plasmon resonance (LSPR) and typically observed for AuNP when excited with light with a wavelength in the Visible-near infrared region (Vis-NIR) of the spectrum [41]. LSPR explain the brilliant color of suspensions of AuNP [2]. For example, when spherical AuNP with a diameter of 18 nm is excited with white light, it appears red as these AuNP absorb the blue and green fractions and leave the red counterpart for external eyes to see. The UV-vis spectrum of the same AuNP typically exhibit a plasmonic absorption maximum around the 520 nm. The optical properties of the same AuNP will significantly change if we change the particle's diameter, shape, refractive index of the medium or the aggregation state. This explains why as suspension of AuNP with a diameter of 100 nm appears blue and not red. For gold nanorods (AuNR), excited electrons have two probabilities to oscillate: (1) around the shorted axis resulting in a transverse plasmon mode with a plasmonic absorption maximum around 520 nm; (2) around the longer axis resulting in a longitudinal plasmon mode with a plasmonic absorption maximum in the far visible to the NIR (650–1200 nm) depending on the ratio of the length to the width of the

AuNR. The strong absorption of AuNR and other anisotropic gold-based nanostructures is highly advantageous for photothermal application considering the deeper light penetration in biological tissue in the NIR region. The absorbed optical energy by AuNP finally decays as a local thermal energy to their close proximity of the excited nanoparticles. For example, cancer cells can be ablated by the uptake of AuNP if excited by the proper light as a result of the generated heat near to the surface of the nanoparticle. It worth to mention that the first clinical trial on human to evaluate the effectiveness of gold-silica nanoshells in ablating prostate cancer were conducted recently and resulted in a promising result [42].

Similar to many other types of inorganic nanomaterials, AuNP could be prepared via top-down or bottom-up approaches [43]. In case of the top-down approach, physical methods are employed to erode a bulk gold into AuNP including laser ablation [44], aerosol technology [45], UV and IR irradiation [46], and ion sputtering [47]. By contrast, synthesis of AuNP via the bottom-up approach starts from the atomic level (gold ions) and builds up to reach nanoparticles at a desired size and shape employing proper chemistries. Chemical techniques to prepare spherical AuNP relies on the reduction of Au ions using proper reducing agents in the presence of capping agents [48]. Currently, these reactions are well established and mechanistic perspectives as well as variables to control the resulting AuNP are well identified. Examples of widely employed chemical protocols to prepare AuNP are the Frens/Turkevich method (for 10–100 nm hydrophilic spherical AuNP) [49,50], the Brust method (for 1–3 nm spherical hydrophobic AuNP) [51], the Murphy/El-Sayed surfactant assisted seed-mediated method (for gold nanorods) [52–55] and the polyol-galvanic method (to prepare gold hollow polyhedral nanoparticles) [56,57]. Other modified protocols and green chemistry-based routes are available in the literature as well [58–61]. Collectively, AuNP enjoy the availability of well optimized, reproducible, tunable synthetic routes to prepare a library of AuNP with various sizes and shapes using simple chemistries. Currently, AuNP with variable size, shape and surface chemistry can be ordered from various commercial suppliers.

AuNP were applied in various biomedical applications including imaging, diagnosis, therapeutics, and drug delivery, as summarized in Figure 1 [35,62–65]. The unique optical properties of AuNP are the origin and the basis of various sensing and imaging applications. For example, the extensive and tunable light absorption of AuNP is the key in the early used lateral flow rapid test strip that are available globally in community pharmacy and in use for six decades to detect and test the level of human chorionic gonadotropic in women's urine. Optical responses upon AuNP aggregation or changing the local refractive index are another bases of many optical-based sensing applications of AuNP. When AuNP aggregate or even de-aggregate, they exhibit extremely different optical properties and this explain why adding salt to ruby red suspension of AuNP turns it quickly to blue upon aggregation. Explanation of these intriguing optical responses and applications in sensing are thoroughly discussed in available review contributions in the literature [66–68].

Away from optical absorption, the extensive elastic light scattering from AuNP can be employed in various optical scattering-based sensing applications. AuNP are excellent light scattering agents in the Vis-NIR and they appear as bright stars under dark field microscopy mode. These optical properties were employed to localize and track these tinny nanoparticles using dark field microscopy [69–71]. Targeted AuNP that can recognize and bind specifically to specific markers on cells and can be used as a reporters to sense and visualize the targeted cells under dark field microscopy [72]. AuNP are excellent enhancers to both fluorescence excitation and vibrational Raman scattering. In fact, fluorophore or Raman active tags experience a tremendous enhancement in their fluorescence and vibrational signals, respectively, if they are placed in the proper distance from AuNP. These enhancements are the bases of many other brilliant sensing platforms and applications and excellent reviews covering these fields are available in the literature [73–77].

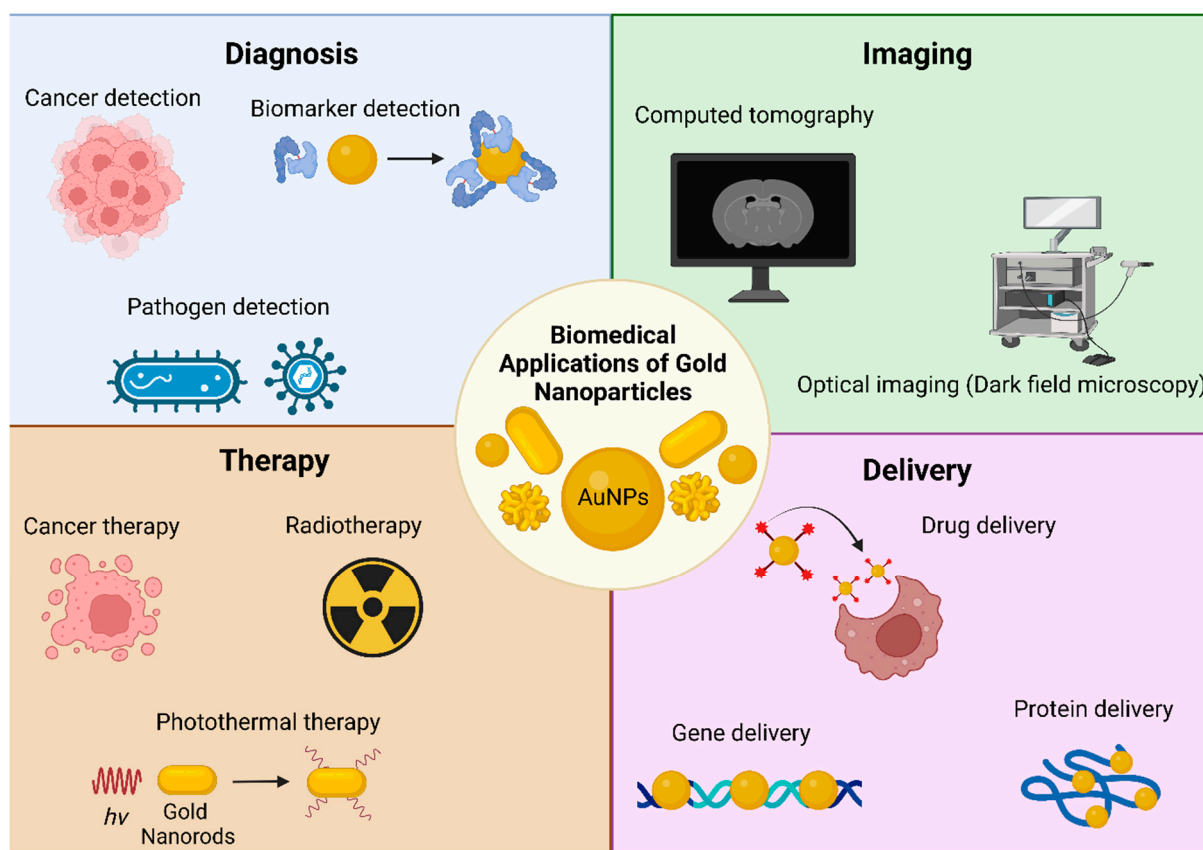


Figure 1. Various biomedical applications of gold nanoparticles as labeled. Figure created in BioRender.com.

Other advantages of AuNP are the ease of visualization using electron microscopy and quantification using mass spectrometry (ICP-MS: inductively coupled plasma-mass spectrometry) with very high sensitivity and low intrinsic background levels in biological samples. We have utilized this attribute to label polymeric nano-host and track their localization inside a single cancer cell [35]. The ease of preparation in various sizes/shapes, surface modification, visualization and quantification make AuNP as “ideal” nanoprobes to understand the fate of nanoparticles, their biodistribution and pharmacokinetics parameters *in vitro* and *in vivo* [14,78].

Anisotropic AuNP that display strong plasmonic absorption in the Vis-NIR and strong photothermal conversion has been explored as potential candidates to fight cancer. The ability to manipulate the surface of these “nano-heaters” is a clear advantage to control their distribution in living organisms and accumulation into cancer regions. From the first pioneering work on utilizing AuNR to ablate cancer cells *in vitro* [79–81] twenty years ago all the way to the recent first clinical trial on human [42], the literature is rich of outstanding reviews on the photothermal effect of gold nanostructures and its fundamentals and applications [11,13,82–90].

3. Liposome Nanoparticles: The Host

In the recent years, liposomes have gained attention from researchers for their potential and diverse applications. In the 1940s, J.Y. Johnson has discovered the first artificially manufactured phospholipid vesicles (i.e., liposomes) for use as model in the pharmaceutical industry [91–93]. In the upcoming years, similar methods for creating liposomes were proposed by different researchers [94,95]. Liposomes are among the first nanocarrier systems to receive FDA-approvals (since 1995 for Doxil[®]) and one of the most biocompatible, convenient and least expensive nanocarrier systems to prepare with true presence in market and clinic [95–98]. Many factors play a major role in the preparation procedure of

liposomes, including lipid and drug concentrations, stirring rate during preparation, and the use of organic solvent/antisolvent [99]. These factors are important to control because they may influence size and number of bilayers (lamellarity) of liposome, which in turn have major effects on drug encapsulation inside the liposomal nanocarrier, release rates an overall pharmacokinetics [91].

Preparation techniques of liposomes are linked with several advantages including their suitability for encapsulating thermo-sensitive drugs, avoidance of using toxic organic solvents, ability to remove the solvent completely, and offering a procedure that is environment-friendly [91,99]. There is a growing need to develop new drug delivery nanocarriers including liposomes because drugs that are marketed in the current pharmaceutical dosage forms are not fully efficient in treating some diseases [100]. Moreover, liposomes have been widely applied throughout the years for delivering hydrophobic drugs with improved bioavailability and controlled release profiles [101]. For instance, docetaxel is known as a very powerful antineoplastic and antiangiogenic agent [102]; however, its clinical applications are limited because of its poor water-solubility and high toxicity [103]. This issue was addressed through loading docetaxel into liposomal nanocarriers, solubilizing the drug, and achieving a controlled drug release formulation [104]. Doxil[®], Myocet[®], and Ambisome[®] are examples of liposomal-based therapies, in addition to many other products that are currently in use in the market [105–109]. Moreover, liposomes are widely applied for biomedical applications since they are biocompatible and biodegradable, have high tissue penetration, can serve as relatively safe drug nanocarriers, and can be manufactured and scaled up using established methods [91,100].

Biomedical applications of liposomes include breast cancer therapy [110], hepatocellular carcinoma [111], cancer Imaging [112], and Rheumatoid arthritis (RA) [113]. However, low solubility of drug-loaded liposomes can result in poor drug loading, high polydispersity of the nanoparticles, and unfeasibility for large-scale production; all these are among the drawbacks linked with the current preparation methods of liposomes [91,99,114]. In the recent years, liposomes gained an increased focus on developing liposome-based nanocomposite complexes that would reserve both exclusive properties of inorganic nanoparticles and the lipidic assembly compromising them [115]. In this regard, many studies tended to develop AuNP-liposome nanocomposites as an attempt to develop effective and potential nanocomposites for future biomedical applications.

4. AuNP-Liposome Nanocomposites: Rationale of Preparation

From material chemistry perspective, nanocomposites are hybrid material that are made of more than one types of materials to combine the advantages of composing components and/or to overcome the limitations/challenges associated with one or more of them [99,116,117]. It is worth to mention that the term “nanocomposite” implies that at least one component to be at the nanoscale. For example, carbon nanofiber and clay nanoplates are employed to reinforce various types of polymers and manipulate their mechanical properties while silver nanoparticles can be doped into textile matrix to provide them with antibacterial properties. Other systems imply the use of two or more materials at the nanoscale such as nano-in nano structures [35,36,118,119], where the discussed system in this review (AuNP-liposome nanocomposites) fall into this category [120–124]. For example, AuNP are poor drug delivery candidates based on the lack of a reservoir or a matrix to load therapeutics. In fact, loading of therapeutics are limited to the surface of the AuNP, and thus the loading capacity is intrinsically less than other nanocarriers (lipidic or polymeric) on weight per weight bases [125]. However, AuNP have excellent optical and thermal properties and has been proven as an excellent light absorber in the UV-vis region of the spectrum with excellent photothermal conversion efficiency to generate local heat that can be employed to fight nearby cancer cells or to induce drug delivery from the hosting matrix. On the other end, liposome nanocarriers in general enjoy a complementing feature such as the ease of therapeutic loading to acceptable loading capacities and efficiencies. In fact, liposomes are one of the first nanoparticles to get FDA approvals

(Doxil[®] in 1995) [108], and has been employed as a carrier for many therapeutics in the clinic [126,127]. Moreover, both hydrophilic and hydrophobic drugs can be loaded into the aqueous reservoir (Doxil[®]) or the bilayer membrane (Ambisome[®]) of the liposome, respectively [108,128]. Considering the features of both AuNP and liposome nanocarriers, it stimulates an interesting approach to prepare nanocomposite of both. One of the early works in this direction described the loading of electron-rich AuNP as a probe into liposomes to enable the visualization of the resulting AuNP-liposome nanocomposite under electron microscopy and thus understanding the liposome-cell interactions [129]. Moreover, encapsulation of AuNP as “nanoprobes” into liposome nanocarriers should help in quantifying the hosting lipid nanocarriers uptake into the cells using inductively coupled plasma mass spectrometry (ICP-MS) analysis. Other driving force is to load NIR-absorbing AuNP into liposomes to enable the fabrication of NIR-responsive lipid nanocarriers that can load therapeutics at acceptable loading capacity and release their payload on demand upon NIR laser irradiation [37,130–132]. In another direction, combining anticancer therapeutics and AuNP in the same liposome nanocarriers might enable synergistic anticancer activity via combining both chemo- and photo-thermal modalities [133]. Finally it is worth to mention that AuNP-liposome nanocomposite can be employed to improve the colloidal and physical stability of both the AuNP and liposomes [134–136]. For example, Runmei et al. have inhibited the aggregation of AuNP through preparing nanosized AuNP-liposome nanocomposite to increase steric hindrance [137]. AuNP modification by phospholipids has been stated to be capable of mitigating the acute cytotoxicity of metallic nanoparticles [138], and manipulating their endocytosis into cells [139]. Lee et al. reported the facile synthesis of AuNP with tunable optical properties inside the aqueous cavity of liposomes and confirmed the improved colloidal stability and cellular uptake of the AuNP-liposome nanocomposite compared to AuNP alone [139]. Collectively, AuNP-liposome nanocomposites would provide a new approach to combine both advantages from liposomes and AuNP, enabling their potential applications in various biomedical fields.

5. AuNP-liposome Nanocomposites: Architectures, Chemistry of Preparation and Analytical Characterization

5.1. Unveiling the Architectures of AuNP-Liposome Nanocomposites

We refer to the term “architecture” herein as the spatial assembly of AuNP and liposomes, which can take various forms: AuNP in the aqueous core of the liposome, AuNP on the outermost shell of the liposome, AuNP in the bilayer or even mixed assemblies. These architectures depend on the size, shape and surface chemistry of AuNP as well as the hosting liposomes and the employed chemistries/methods to prepare the nanocomposites. The starting materials for AuNP in the AuNP-liposome nanocomposites can be either pre-prepared AuNP or gold ions that need to be reduced in-situ. Hydrophilic pre-prepared AuNP can be assembled on the outermost layer of the liposomes (Figure 2A) if enough attractions (electrostatic or covalent) are provided [140]. If a suspension of the Hydrophilic pre-prepared AuNP was used as the hydration media to prepare the liposomes (details follow in next sections), AuNP can be encapsulated into the aqueous core as demonstrated in Figure 2B [141]. Alternatively to using pre-prepared hydrophilic AuNP, ionic or molecular precursors of gold can be used as a starting material followed by the successful encapsulation of these precursor into the aqueous cores of liposomes and ultimately the reduction into AuNP [139]. Hydrophobic pre-prepared AuNP can be incorporated into the bilayer membrane as shown in Figure 2C [142] for ultrasmall AuNP with a diameter approaching the lipid membrane thickness (about 3–5 nm) and capped with hydrophobic capping agent (i.e., alkanethiols) [142,143]. From this discussion, it is apparent that the spatial assembly of AuNP “in or on” liposomes can be achieved via controlling the properties of AuNP (hydrophilicity, size and surface charge) as well as the employed method of preparation as we will detail in the next section.

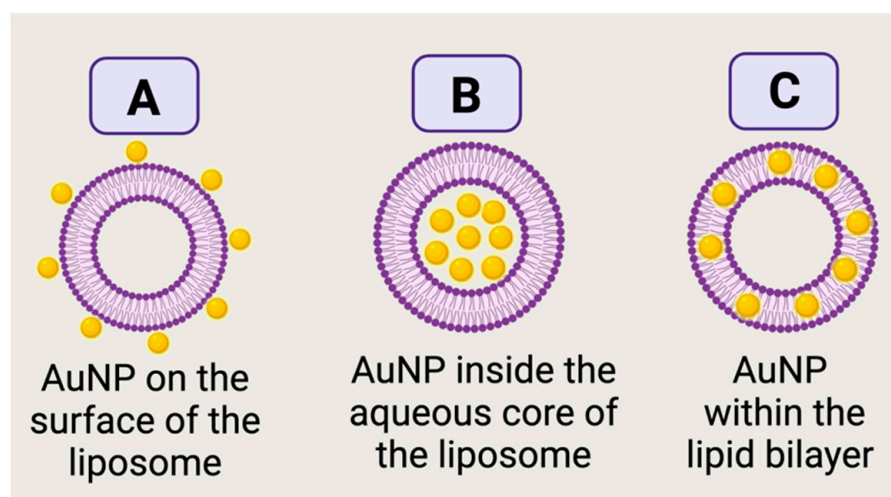


Figure 2. Illustration of different architectures of AuNP-liposome nanocomposites. Pre-prepared hydrophilic AuNP on the outermost shell (A) or in the aqueous reservoir (B) of a liposome. In (C), pre-prepared ultrasmall hydrophobic AuNP are embedded in the bilayer of a liposome. Figure created in BioRender.com.

5.2. Chemistries to Prepare AuNP-Liposome Nanocomposite

Before we discuss the available chemistries to prepare AuNP-liposome nanocomposites, it is important to discuss briefly the preparation of the hosting liposome followed by a discussion related to when and how AuNP can be introduced. Typical formation of liposomes via thin film hydration method is shown in Figure 3 [144]. Briefly, the thin film hydration method implies the dissolution of lipids in a volatile organic solvent, followed by rotary evaporation of the solvent to form dried lipid film. Further, the lipid film swells by hydration in an aqueous medium and multilamellar vesicle starts to form. To obtain, uniform unilamellar vesicles, the suspension is passed through a polycarbonate filter with defined pore size [145]. AuNP can be introduced at different stages. Figure 3A, shows the introduction of pre-prepared hydrophilic AuNP as an aqueous suspension to hydrate the dried lipid film, which results in the encapsulation of AuNP into the aqueous core of the formed liposomes. Figure 3B, shows the introduction of AuNP at much later stage, where the liposome is already formed and thus the resulting architecture will be mostly assembled AuNP on the liposome outer shell (i.e., covalent or electrostatic binding). Chemistries described in Figure 3 requires hydrophilic AuNP with size typically smaller than the size of the liposome and typically results in poor encapsulation yield [139]. After the formation of AuNP-liposome nanocomposite, unencapsulated AuNPs could be removed using several purification methods including repeated slow-speed centrifugation or density-based fractionation [37,146,147].

For hydrophobic AuNP with small size (i.e., alkanethiol-capped AuNP with diameter less than 5 nm), AuNP can be introduced in the first step and suspended in the organic solvent with the dissolved phospholipid as shown in Figure 4. Upon drying, phospholipid and hydrophobic AuNP will form a dried film, which upon hydration will result in liposome that encapsulate the small AuNP in the bilayer membrane [142]. It is worth to mention that this protocol can only be applied for small AuNP that individually do not exhibit optical properties in the Vis-NIR [148,149]. Moreover, the incorporation of AuNP in the bilayer may result in significant impact on the stability of the hosting liposome and fragmentation into micelles [139]. Furthermore, the fundamental drawback of this technique is that it possesses low encapsulation efficiency, which necessitates an extra step for removing the free AuNP [109]. In addition, drug incorporation after liposomal preparation was correlated with higher encapsulation efficiency compared to drug incorporation during the liposomal formation, which guarantees improved drug bioavailability in the targeted site of action [94]. It is noteworthy to mention that the choice of the material incorporation (i.e.,

either after or during liposomal formation) depends on several standards, including the properties of the incorporated material (i.e., hydrophilic or lipophilic), the targeted profile of the drug release, and therapeutic applications of the prepared liposome-based nanocomposite [150–154]. Although production methods of liposome-based nanocomposites received significant efforts for scaling-up these fabrication techniques, some concerns include the poor colloidal stability profile, low encapsulation efficiencies, toxicity coming from the organic solvents used during synthesis process, and high costs of large-scale fabrication are associated with the production of liposome-based nanocomposites [94]. However, these limitations are variable based on the production techniques followed during the liposomal formation process. In other words, some liposome production methods (i.e., Freeze Drying, Reverse-Phase Evaporation, and Membrane Contactor) are among the useful techniques that are efficient for large-scale fabrication of liposome-based nanocomposites.

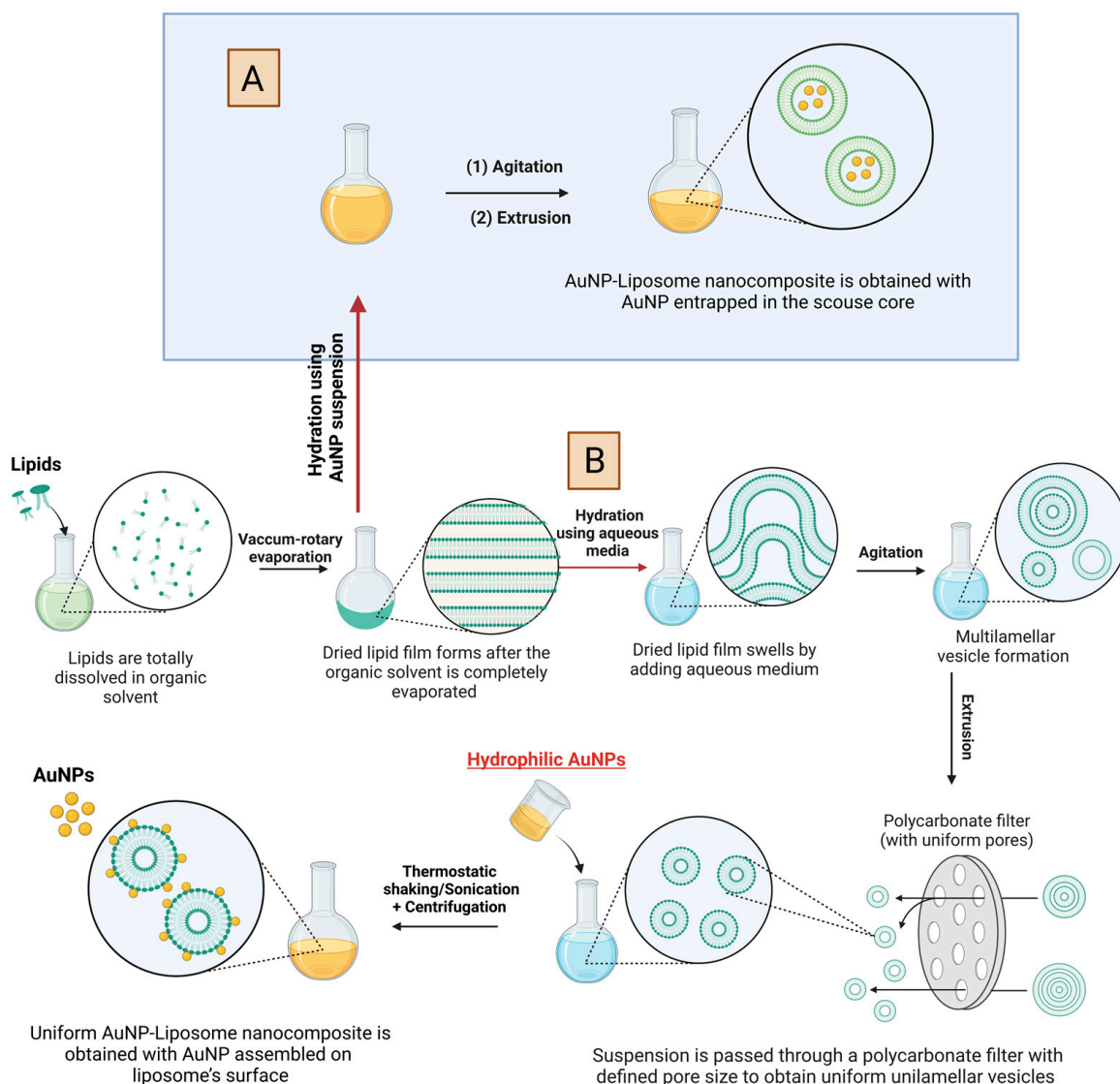


Figure 3. Schematic illustration of the preparation of AuNP-liposome nanocomposite using hydrophilic AuNP. Note that the preparations of two different architectures are sketched: AuNP in the aqueous core of the liposomes (A) and AuNP on the outermost shell of the liposome (B). For the later, attractive forces (electrostatic or covalent interaction) should exist for stable assembly. Figure created in BioRender.com.

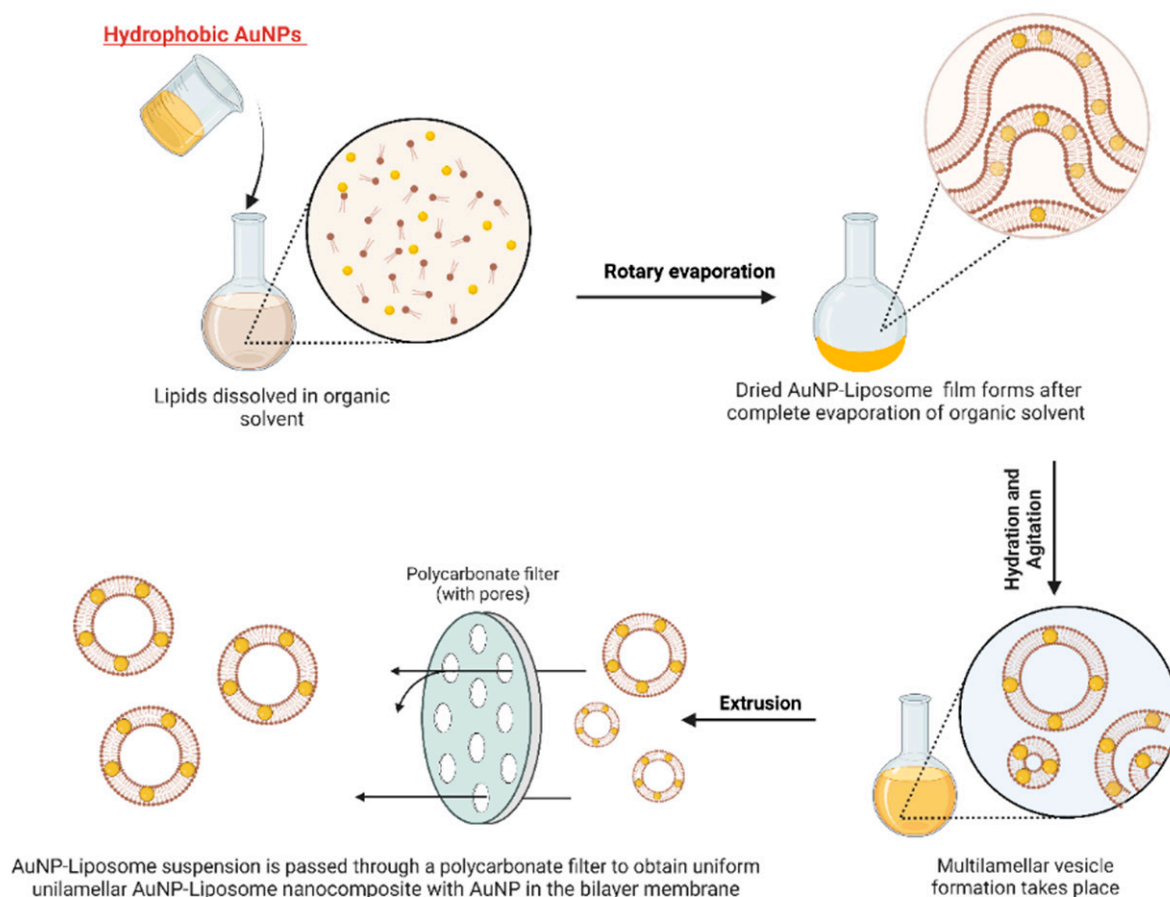


Figure 4. Schematic illustration of the preparation of AuNP-liposome nanocomposite using ultra-small hydrophobic AuNP. Note that the resulting architectures implies the incorporation of AuNP into the lipid membrane bilayer. Figure created in BioRender.com.

Alternatively, liposomal dried film can be rehydrated with a reducing agent and then gold ions can be introduced and selectively reduced inside the aqueous core of the liposomes as shown in Figure 5A, which could be called in-liposome reduction approach [139]. Lee et. al. utilized this approach with sodium citrate or ascorbic acid as reducing agents and tetrachloroaurate ions as the gold precursors, while the reduction was carried out at room temperature overnight. Employing the in-liposome reduction approach, the research group prepared seven types of AuNP-liposome nanocomposites with tunable size, metal compositions and optical properties [139]. On-liposome reduction approach is another pathway where gold undergoes reduction on the surface of pre-synthesized liposomes (Figure 5B) [122]. Table 1 summarizes the reported chemistries used to prepare AuNP-liposome nanocomposites and the physiochemical properties of each component and the resulting products.

In the preparation of AuNR, shape-directing agents (i.e., CTAB) are used to promote the anisotropic growth of AuNR. Unfortunately CTAB has cytotoxic profile which limits the biomedical applications of CTAB-capped AuNR [155–157]. In this regard, Gudlur et al. reported the CTAB-free preparation of AuNR using cationic liposomes as a substituent for the CTAB in order to improve the biocompatibility of AuNR [158]. The authors used cationic pre-prepared liposomes that were mixed with gold precursor (HAuCl_4) in the presence of silver salt, reducing agent (ascorbic acid), and followed by heating at 40 °C to prepare anisotropic AuNR-liposome nanocomposite. Interestingly, AuNR-liposome nanocomposite potentially induced a significant photothermal ability by hyperthermia-induced cell death in different cancer cell lines, and thus resulting in enhanced cellular uptake compared to CTAB-mediated AuNR. However, the actual role of liposomes in the

synthesis process of AuNR is still unknown, and much research needs to be conducted to validate this emerging method.

Table 1. Examples of reported AuNP-liposome nanocomposites.

AuNP Characteristics	Nanocomposite Preparation Chemistry	Nanocomposite Characteristics	Outcomes and Remarks	References
<ul style="list-style-type: none"> Sodium citrate or ascorbic acid as reducing agents 	<ul style="list-style-type: none"> Liposomes encoded with the reducing agent were resuspended in the gold precursor to form AuNP-liposome by electrostatic attraction 	<ul style="list-style-type: none"> Size of 28–161 nm Spherical shape Enhanced colloidal stability 	<ul style="list-style-type: none"> Selective encapsulation of reducing agent in to liposomes allows self-crystallization of AuNP within the liposome 	[139]
<ul style="list-style-type: none"> 10–50 nm with Glycerol as a reducing agent Stable AuNP for two months without an added stabilizer 	<ul style="list-style-type: none"> AuNP were covalently immobilized on the thiol-functionalized surface of the liposome prepared by thin film hydration method 	<ul style="list-style-type: none"> Size of 190 nm Spherical shape 	<ul style="list-style-type: none"> The percentage of glycerol has no influence on the size and the polydispersity index Possible immuno-sensing applications 	[140]
<ul style="list-style-type: none"> 25 nm PEGylated using Polyethylene glycol Zeta potential of −29.6 mV 	<ul style="list-style-type: none"> Cationic liposomes prepared by thin-layer evaporation method were decorated using anionic PEGylated AuNP using electrostatic interactions 	<ul style="list-style-type: none"> Size of 180–389 nm Zeta potential of 43–51 mV 	<ul style="list-style-type: none"> Potential biomedical applications related to drug delivery 	[159]
<ul style="list-style-type: none"> 6 nm capped with Cetyltrimethylammonium bromide (CTAB) 	<ul style="list-style-type: none"> Negatively charged liposomes prepared by thin film hydration method were electrostatically bound to the positive AuNP 	<ul style="list-style-type: none"> Size of 177.3 nm Zeta potential of 4.4 mV 87.44% loading capacity of doxorubicin inside the AuNP-liposome nanocomposites 	<ul style="list-style-type: none"> Possible application for cancer therapy 	[160]
<ul style="list-style-type: none"> 19 nm capped with procyanidin 	<ul style="list-style-type: none"> Negatively charged AuNPs were electrostatically bound to the positively charged liposomes prepared by thin film hydration method 	<ul style="list-style-type: none"> Size of 200–350 nm zeta potential of −26.01 mV Spherical shape Stable profile after AuNP incorporation Excellent light-controlled drug release 	<ul style="list-style-type: none"> Combination between Doxorubicin-loaded AuNP-liposome nanocomposites and laser irradiation supports their medical application for cancer therapy 	[161]
<ul style="list-style-type: none"> Sodium citrate as a reducing agent Functionalized with carboxyl groups and silver 	<ul style="list-style-type: none"> Negative AuNP were covalently linked (using EDC and NHS) * to the positive amino-modified liposomes surfaces prepared by thin film hydration method 	<ul style="list-style-type: none"> Size of 215.5 nm Zeta potential of −11.6 mV 90% encapsulation of Doxorubicin with increased drug release under laser stimulation 	<ul style="list-style-type: none"> Potential biomedical applications related to cancer therapy 	[162]
<ul style="list-style-type: none"> 14.1 nm coated with Citrate 	<ul style="list-style-type: none"> Negative AuNP were electrostatically adsorbed onto the zwitterionic liposome surface by the gel-liquid phase transition of the lipid membrane 	<ul style="list-style-type: none"> Size of 105 nm Stable size over 1 week of incubation at room temperature Spherical morphology 	<ul style="list-style-type: none"> Protecting agents possess a key factor on linear self-assembly of AuNP within the liposome surface 	[163]
<ul style="list-style-type: none"> Size of 2–8 nm with ascorbic acid as a reducing agent 	<ul style="list-style-type: none"> In situ reduction of AuNP on the liposome surface 	<ul style="list-style-type: none"> Size of 100–120 nm Spherical shape 	<ul style="list-style-type: none"> Biodistribution studies confirm no cytotoxic profile of the AuNP-liposome nanocomposites 	[122]

Table 1. Cont.

AuNP Characteristics	Nanocomposite Preparation Chemistry	Nanocomposite Characteristics	Outcomes and Remarks	References
<ul style="list-style-type: none"> Size of 20–40 nm with sodium citrate as a reducing agent 	<ul style="list-style-type: none"> AuNP were noncovalently encapsulated inside liposomes prepared by thin film hydration method 	<ul style="list-style-type: none"> Size of 60–80 nm Spherical shape Zeta potential of -10.4 mV 	<ul style="list-style-type: none"> Induction of time and dose dependent death of breast cancer cells 	[164]
<ul style="list-style-type: none"> Ascorbic acid as a reducing agent 	<ul style="list-style-type: none"> In situ reduction of positive AuNP on the negative liposome surface prepared by thin film hydration method 	<ul style="list-style-type: none"> Size of 100–150 nm Spherical shape Zeta potential of 20 mV 	<ul style="list-style-type: none"> Potential biomedical applications for acne treatment 	[165]

* EDC: 1-ethyl-3-(3-dimethylaminopropyl)carbodiimide; NHS: N-hydroxysuccinimide.

5.3. Analytical Characterization of AuNP-Liposome Nanocomposites

Transmission electron microscopy (TEM) is a typical tool to visualize the architecture of AuNP-liposome nanocomposites and confirm the spatial distribution of AuNP whether on the outermost shell of the liposome (Figure 6Ai), inside the aqueous core (Figure 6Aii), or within the liposome bilayer (Figure 6Aiii). However, negative staining is usually required, and thus staining-related artifacts are possible challenge. Another challenge is related to the two-dimensional nature of the TEM imaging, which makes it difficult to confirm if the nanoparticles are “on” or “in” the liposome. A more complex tool is the Cryogenic transmission electron microscopy (Cryo-TEM), where thin film of liposome suspension is frozen under liquid nitrogen temperature [166]. The resulting vitrified ice film is extremely thin and can be imaged directly by EM (Figure 6Aiv). Alternative indirect method is the use of the sodium cyanide test, in which the successful coating of the AuNP with lipids can be tested using the oxidation capacity of cyanide to the encapsulated AuNP and the protection role of the lipid bilayer [167]. In this assay, the lipidic shell that coats the AuNP surface acts as a non-ion-permeable barrier that protects the golden core from exposure to cyanide ions as shown in Figure 7. For encapsulated AuNP, addition of cyanide will prevent or delay the oxidation of the protected AuNP, and thus the original color of the suspension will be maintained compared to control naked AuNP [167]. If AuNP is “on” the liposome or simply suspended in the same media without effective encapsulation, then added cyanide can oxidize the AuNP and the suspension color will disappear. Moreover, brilliant color of nanogold and its unique plasmonic optical extinction in the Visible-NIR region of the spectrum can be followed to confirm the formation of AuNP-liposome nanocomposites (Figure 6B,C) [130]. Coloration of liposome is a visual evidence supporting the formation of AuNP-liposome nanocomposites. Elemental analysis using energy dispersive spectroscopy (EDS) can be employed to further support the formation of AuNP-liposome nanocomposites, looking for the gold fingerprints as shown in Figure 6D [133]. Quantitatively, gold content can be measured using inductively coupled mass spectrometry (ICP-MS) and reported as weight percent of the nanocomposite (Figure 6E) [168]. The various analytical modalities that can be used to confirm the presence, quantify and visualize the encapsulated AuNP are justifications to use AuNP as labels for liposomes, and thus to understand the biological interactions and fate of labeled liposomes. It is noteworthy to highlight the need to compare information gathered by complementary techniques to confirm the properties of the prepared AuNP-liposome nanocomposites. For instance, morphological information obtained from SEM and TEM could be further correlated with the optical absorption spectra of the nanocomposite where coloration of liposomes and AuNP and its unique plasmonic optical extinction in the Visible-NIR region could confirm the formation of the AuNP-liposome nanocomposites and its size that correlates with unique wavelengths [122,130,169]. Moreover, correlating the data obtained by FTIR, XPS, and ICP-MS could provide insights on the overall structure, composition, and surface properties of the AuNP-liposome nanocomposites [133,170].

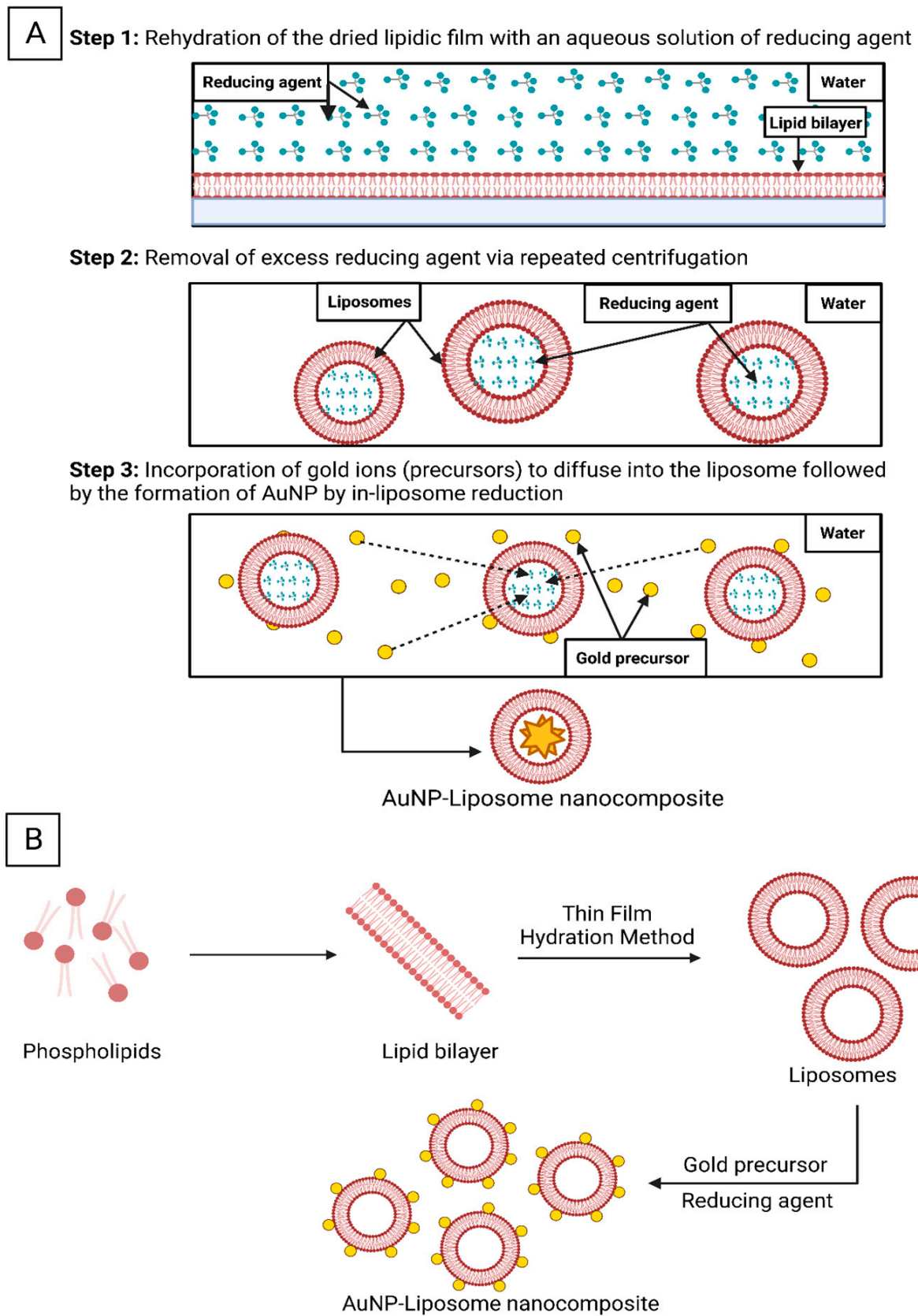


Figure 5. Schematic illustration of the AuNP-liposome nanocomposites formation using the “in-liposome” (A) and “on-liposome” (B) reduction approaches. Figure created in BioRender.com.

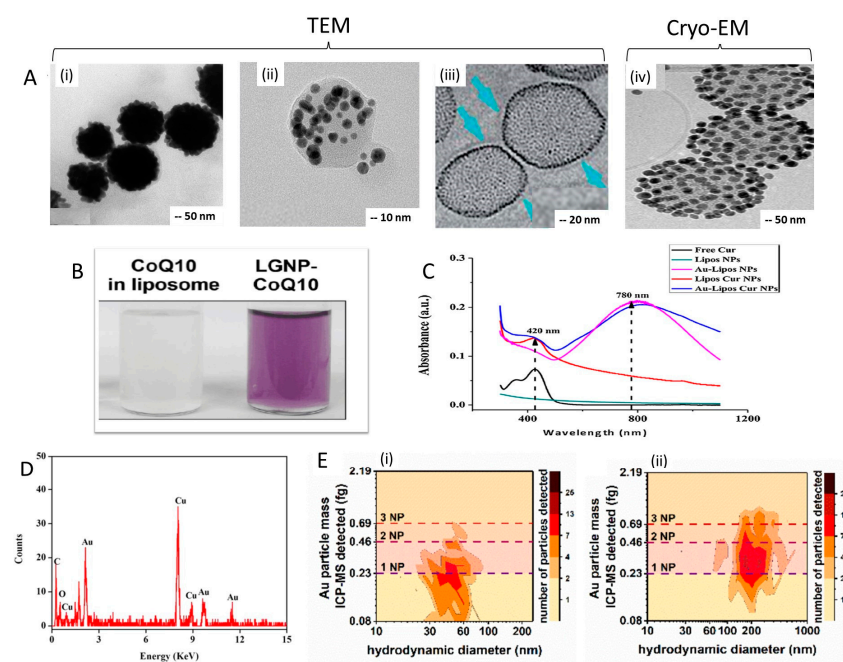


Figure 6. (A) TEM images of (i) AuNP-surface coated liposomes, (ii) AuNP-Loaded liposomes, (iii) AuNPs within the liposomal bilayer, and (iv) Cryo-EM images of AuNP-surface coated liposomes. (B) Successful incorporation of AuNP is evident from the development of violet color in the liposome suspension. (C) Absorption spectra of free drug, empty liposomes and AuNP-liposome in aqueous environment illustrating the differences in the Vis-NIR absorbance upon AuNP incorporation. (D) Elemental analysis of AuNP-liposome nanocomposites. (E) Spike fractograms from ICP-MS reporting the detected AuNP mass and indicating (Ei) AuNP particle size of 30 nm, and (Eii) AuNP-liposome size around 200 nm. (A) Reproduced with permission from (i) [122], copyright Frontiers 2015, (ii) [164], copyright IOP Publishing Ltd. 2018, (iii) [171], copyright The Royal Society of Chemistry 2012, and (iv) [172], copyright Elsevier 2009. (B) Reproduced with permission from [169], copyright PLOS 2020. (C) Reproduced with permission from [130], copyright Elsevier 2018. (D) Reproduced with permission from [133], copyright IOP Publishing 2018. (E) Reproduced from [170].

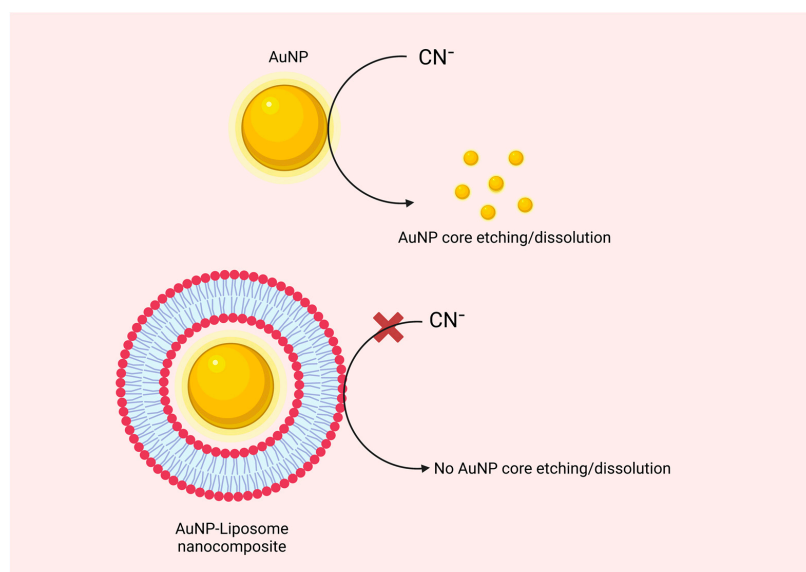


Figure 7. Graphical illustration of the protective properties of the AuNP encapsulated into the liposomal core against chemical etching with cyanide ions. Figure created in BioRender.com.

6. Biomedical Applications of the AuNP-Liposome Nanocomposites

Due to their unique “combined” properties we have discussed thus far, AuNP-liposome nanocomposites have been evaluated for several biomedical applications including imaging, sensing, cancer therapy, and light-responsive drug delivery. The following discussion will highlight these applications in brief with selected examples from the literature.

6.1. Imaging

The employment of gold in biomedical imaging is attributed to its ability to exhibit unique optical imaging properties and being excellent contrast for TEM-based and X-ray based imaging. For instance, Sanzhakov et al. have developed a AuNP-liposome nanocomposites for tumor imaging [33]. The accumulation of AuNP-liposome nanocomposite was tracked in mice using computed tomography (CT) scanner to evaluate the contribution of targeting moiety on the uptake into tumor in vivo and to confirm that PEGylation of AuNP-Phospholipid nanocomposite improves the accumulation of AuNP in the tumor site (Figure 8). In another study, AuNP-liposome nanocomposite (150–200 nm) have been prepared and illustrated a good CT contrast with better signals compared to commercially available AuNP (15 and 40 nm) (Figure 8), and thus proposing a novel approach for cancer imaging [173]. Similarly, the signal from AuNP-liposome nanocomposite was strong and stable inside the tumor after injection, signifying the potential stability and tissue retention of the construct [174,175].

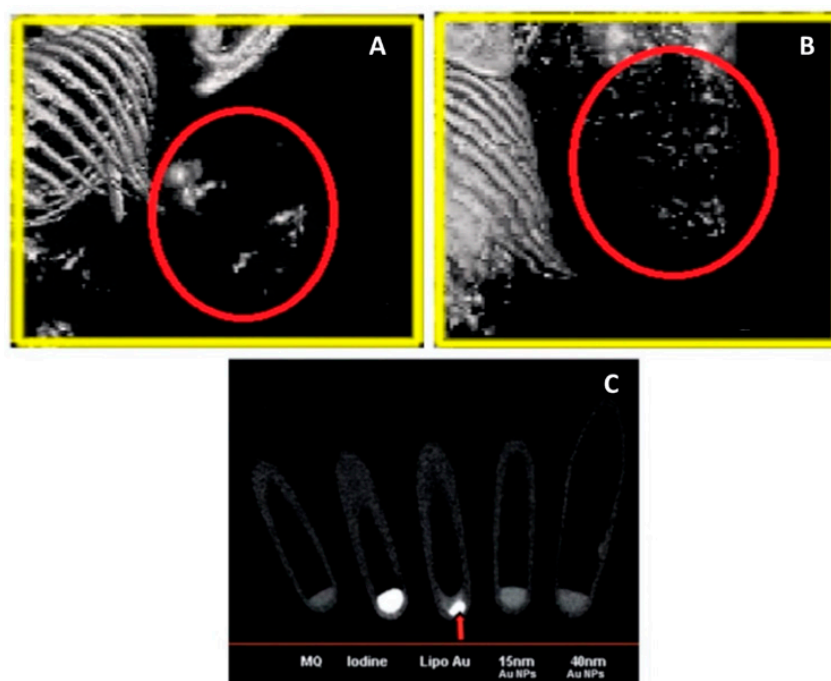


Figure 8. CT of laboratory mice with Lewis lung carcinoma after intravenous administration of AuNP-Phospholipid nanocomposite in the presence (A) and absence (B) of Poly (ethylene glycol)-distearoylphosphatidylethanolamine (PEG-DSPE) after 90 minutes illustrating a significant gold accumulation in the tumor site from the PEGylated AuNP-Phospholipid nanocomposite compared to the non-PEGylated nanocomposite (shown in the red circles). (C) X-ray CT imaging of AuNP-liposome (shown in the arrow) illustrating a superior CT contrast signal compared to the generated signal from the commercially available gold seeds. (A,B) Reproduced with permission from [33], copyright Elsevier 2021. (C) Reproduced with permission from [173], copyright RSC Publishing 2013.

6.2. Sensing

AuNP have been widely applied in biosensing for biomedical purposes including DNA hybridization [176,177], DNA–protein interactions [178,179], and cell transfections [180,181] due to their optical properties, their simple preparation techniques, and the ease of surface modification. Currently available detection techniques for bacteria, primarily nucleic acid-based methods, could achieve low detection limits. In this regard, a simple and nanoscale assay based on AuNP-liposome nanocomposites was developed for bacterial detection purposes [182]. For example, a simple colorimetric assay based on AuNP-liposome nanocomposites was developed to detect bacterial toxins. For example, Listeriolysin (LLO) is a toxin produced by the bacterium *Listeria monocytogenes* and acts primarily on lipid membranes to induce pores. Liposomes loaded with cysteine were used as the natural recognition element in this assay, in which the presence of LLO induces the liberation of cysteine from liposomes, and consequently induce aggregation of the suspended AuNP resulting in a strong optical response (a colorimetric transformation from red to purple/blue) as demonstrated in Figure 9. The intensity of the produced color correlates with the LLO concentration, and thus, proposing a simple and rapid quantitative nanoscale assay for further development of portable sensors. In a similar colorimetric assay-based attempt, amine-functionalized AuNP-liposome nanocomposite was fabricated as an attempt to detect thrombin molecule by triggering a color change from blue to red [183]. The employed AuNP-liposome nanocomposites possessed an improved sensitivity by almost 3 folds in the existence of AuNP compared with the condition without AuNP. As an attempt to enhance the plasmonic biosensing using AuNP-liposome nanocomposites, detection of the bacterial toxin has significantly improved reaching a limit of detection (LOD) of 0.1 ng/mL [184]. Moreover, the proposed nanocomposite illustrated strong properties for optical biosensing as well as demonstrating a long shelf life, and conserved efficiency for over four weeks. Additionally, a unique AuNP-liposome nanocomposites was proposed for electrochemical investigation of lipopolysaccharide in food samples in which it plays a role as a signal amplifier, a signal output component and a molecular recognizer [185].

6.3. Phototherapy and Laser-Triggered Drug Delivery

Perhaps, the strongest justification and greatest interest for preparing AuNP-liposome nanocomposites is the preparation of laser-triggered drug release systems and combining chemotherapy from loaded therapeutics with photothermal effect from the excited AuNP. First, AuNP are optically active and exhibit strong photothermal conversion efficiency in the NIR as discussed in previous sections. However, AuNP has poor intrinsic drug loading capability due to the absence of reservoir or matrix for loading. At the other end, liposomes are excellent carriers for vast range of therapeutics with proven biocompatibility and presence in clinics. The fabrication of AuNP-liposome nanocomposites should bring the best of both: (1) excellent drug loading into the liposomes and (2) light responsiveness which can trigger the release of loaded therapeutics. Excellent examples are reported in the literature using various types of liposomes and AuNP [123,124,186–188]. This approach was first reported in 2007 by Lauri and co-workers who encapsulated hydrophilic and hydrophobic AuNP into the lipid bilayer or the aqueous reservoir of liposomes, respectively [124]. At physiological temperature, the AuNP-liposome nanocomposites remained intact while upon irradiation, a rapid release of the encapsulated fluorescent marker was observed. It is important to note that in this novel and one of the first proof of concept evaluations, UV light was employed which is not preferred for biomedical applications as the tissue penetration at this wavelength is poor. In 2008, Zasadzinski and co-workers prepared an NIR-responsive AuNP-liposome nanocomposites using hollow gold nanoshells (HGN) [189]. Interestingly, the triggered release rate was dependent on the attachment route of HGN to liposomes (in-liposome, on-liposome or even freely and independently outside the liposomes), the laser power and the irradiation time. The mechanism of release upon laser irradiation was explained by the microbubble formation upon heating and the resulting lipid membrane disturbance and fragmentation of the liposomes. Following these

two pioneering works, many research groups reported the use of light-responsive AuNP-liposome nanocomposites both *in vitro* and *in vivo* (Figure 10) [37,121,122,132,190,191]. Indeed, combination of AuNP and liposome is not only a tool to induce a triggered drug release, but to achieve synergistic anticancer activity. For example, Gao and co-workers reported a synergistic antitumor effect in tumor-bearing mice from combining wedelolactone (loaded anticancer agents into the liposomes) and NIR-absorbing AuNP and reported up to 95.73% inhibition rate (Figure 11) [192]. Away from light, AuNP-liposome nanocomposite can be fabricated to trigger their payload therapeutics in the presence of other stimuli. For example, bacterial toxins were utilized to deliver antimicrobial agents specifically to the sites of bacterial infections [34].

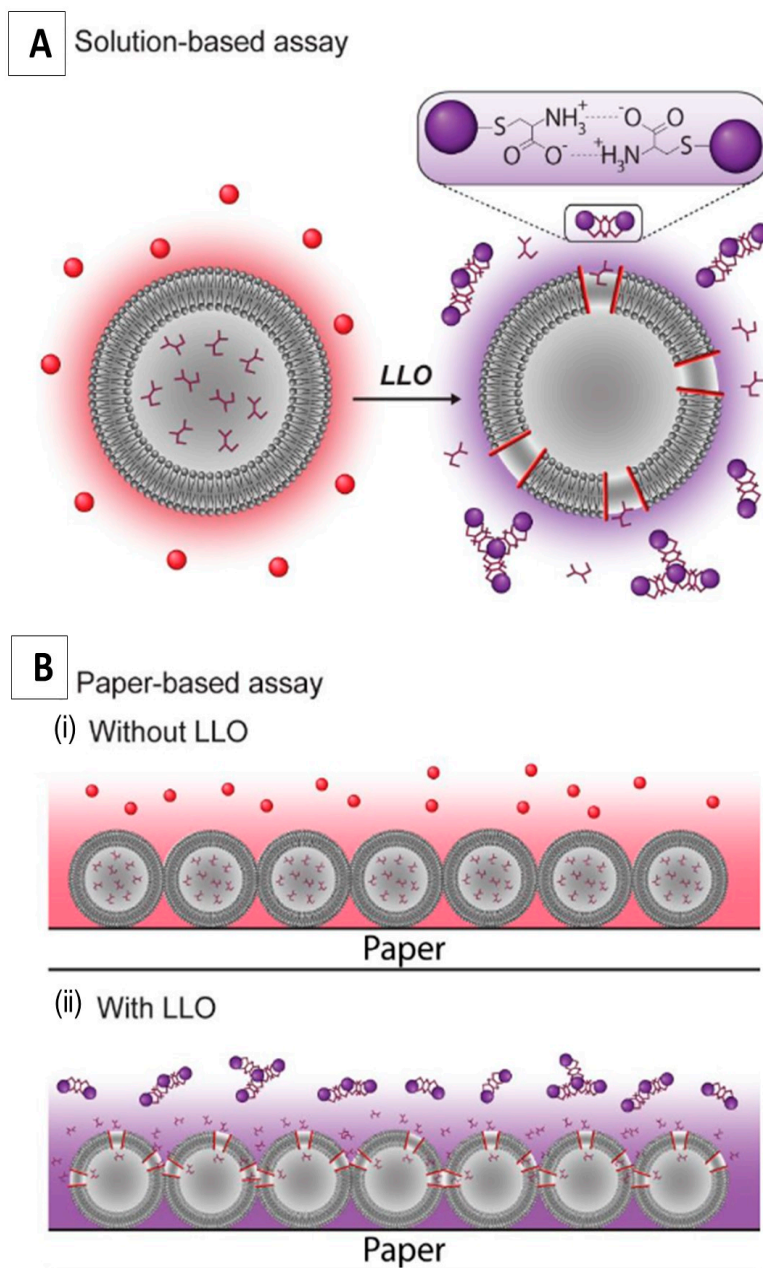


Figure 9. Graphical illustration of the solution-based (A) and paper-based (B) Assays for detecting the Pore-Forming Toxin Listeriolysin O (LLO). Adapted with permission from [182], copyright American Chemical Society 2020.

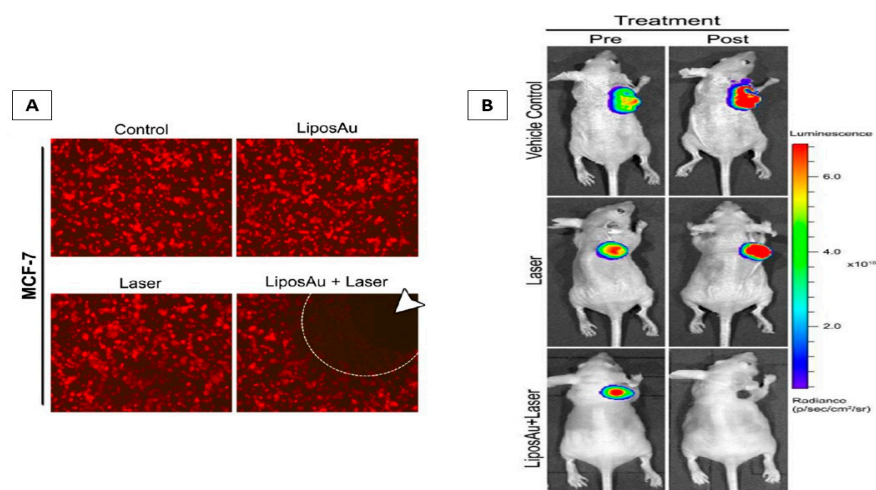


Figure 10. (A) Fluorescent micrograph images of the photothermal-mediated therapy using AuNP-liposome nanocomposites and laser against MCF-7-fluc2-turboFP tumor cells (absence of red color represents cell death as shown by the arrow). (B) Pre- and post- injecting liposome-AuNP nanocomposite treatment bioluminescence images of mice bearing HT1080-fluc2-turboFP tumor xenograft showing the significant tumor suppression from the combined photothermal and chemothermal treatment. (A,B) Reproduced with permission from [122], copyright American Chemical Society 2015.

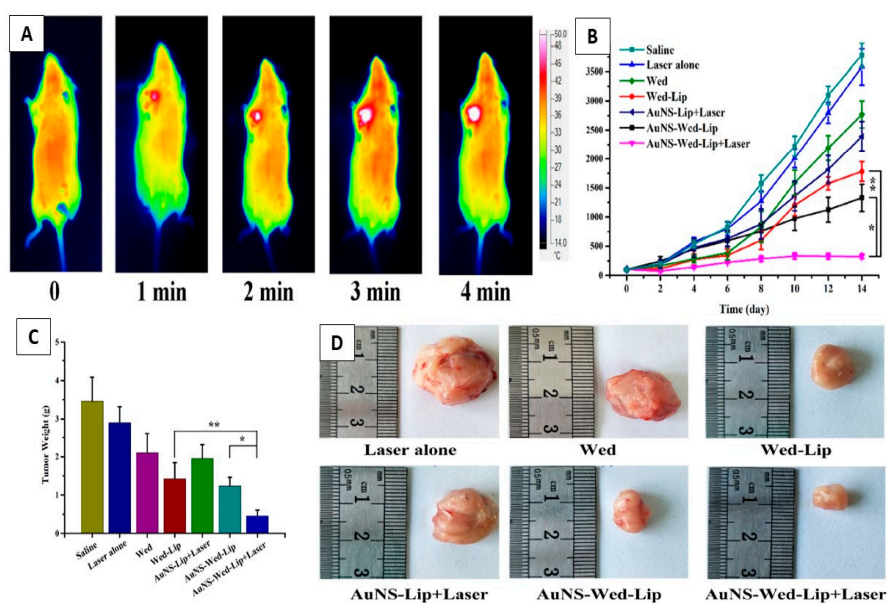


Figure 11. (A) Thermal images of tumor-bearing mice after exposure to NIR irradiation and injection with wedelolactone (anticancer agent) loaded AuNP-liposome nanocomposites. (B) Changes in the tumor volume in the tumor-bearing mice in different treatment groups. (C) Weights of the tumor in different treatment groups (* means $p < 0.05$ and ** means $p < 0.01$). (D) Images showing the removed tumors from the mice bearing S180 tumor after 2 weeks of treatment. All graphs were reproduced with permission from [192], copyright Elsevier 2019.

7. Biodistribution and Pharmacokinetics of AuNP-Liposome Nanocomposites

The fate of AuNP is significantly influenced by their physiochemical characteristics such as size, shape and surface chemistry [193]; thus, tuning these properties during fabrication could earn it the desired biodistribution and pharmacokinetics profile. The non-specific adsorption of plasma proteins (opsonization) to AuNP [194] and subsequent recognition and elimination by the reticuloendothelial system (RES) are among the main challenges in achieving the desired biodistribution profile [195]. The instant uptake from the plasma by

the immune system when administered intravenously affects their residence time in blood circulation, and thus their therapeutic function. Hence, an effective strategy to preserve the nanoparticle characteristics and enhance its biodistribution and pharmacokinetics profile is desired. Zhang et al. reported the preparation of AuNP-liposome nanocomposites in ‘cluster bomb’ structures with unique load release pattern as an effective strategy to improve the pharmacokinetic properties of loaded paclitaxel (PTX) [196]. This system can be visualized as a hybrid system in which a part of PTX was covalently linked to AuNP (slow-release carrier) and another part was physically encapsulated into the liposome carrier (fast release carrier). The ratio of free to covalently attached PTX was simply tuned by mixing liposome encapsulating free PTX and PTX-conjugated AuNP. This nanocomposite exhibited a “burst” release of PTX from liposomes in the site of action and maintained a slower release rate from the PTX-conjugated AuNP. The described “multi-order” release of PTX enabled rapid C_{max} values and steadily elevated AUC_{0-t} values. This example demonstrates the added benefit of preparing a hybrid system of AuNP and liposome to tune the pattern and rate of drug release, and thus to control the collective pharmacokinetics of therapeutics.

The clearance of AuNP and generally inorganic nanoparticles is determined mainly by their size (Figure 12). Small size particles of less than 5.5 nm (a molecular weight of approximately less than 50 kD) stay in the circulation for a shorter duration due to the renal glomerular filtration process into urine [197]. As shown in Figure 12, incorporating small AuNP (i.e., 20 nm as shown in a red rectangle in Figure 12) into larger liposomes (i.e., 150 nm as shown in a red rectangle in Figure 12) shift very significantly the hybrid system’s clearance (mainly hepatic) by ten folds. Hence, encapsulated AuNP are protected from clearance and stay in circulation for longer periods of time, which could reach up to 14 days [122,198]. Upon the degradation of AuNP-liposome nanocomposites, the resulting smaller AuNP particles could then be eliminated by renal routes (if they are less than 5.5 nm in diameter). Rengan et al. reported the preparation of biodegradable NIR-responsive AuNP-liposome nanocomposites by the “on-liposome” reduction method discussed in previous sections. Their synthesis resulted in the formation of “golden shell” that is composed from assembled ultrasmall AuNP (2–8 nm in diameter) that support collectively the photothermal effect in the NIR [122]. Remarkably, the described hybrid system liberated ultrasmall AuNP upon degradation, which was renally eliminated as confirmed in vivo by ICP-MS analysis of urine.

Another factor that has been shown to influence the clearance of AuNP-liposome nanocomposites systems was the surface charge. For example, cationic AuNP-liposome nanocomposites system, coated with positively-charged 1,2-dipalmitoyl-sn-glycerol-3-phosphocholine (DPPC), exhibited enhanced excretion of AuNP-liposome through the negatively charged glomerular basement membrane and gold was detected in urine. This charge repulsion mechanism in the kidney controls the filtration of molecules, in which those with a negative charge are repelled; while the positively charged molecules are filtered [122,199].

Generally, once AuNP are injected intravenously, they are captured by RES through macrophages and delivered to the liver, spleen, and lungs. Various approaches were employed to provide a stealth character to AuNP including modification of the nanoparticle’s surface with PEG, zwitterionic ligands, cell membranes and proteins [200–202]. Recently, liposomes were proposed as a carrier to alter the cellular uptake, biodistribution and pharmacokinetics of AuNP. For example, Nam et al. [203] and Zhang et al. [196] prepared pegylated AuNP-liposome nanocomposites in order to prolong their circulation. Although PEG-AuNP-liposome nanocomposites were able to escape the immune system, in vivo experiments demonstrated the majority of the injected dose accumulated in the liver and spleen, but in 1.5 folds lower concentrations than the conventional AuNP.

Overall, different formulations of AuNP-liposome nanocomposites revealed different kinetics than the conventional AuNP. AuNP-liposome nanocomposites synthesized with biodegradable lipid accumulate gradually in the liver and are subjected to biological degradation by lipid enzymes resulting in losing the spherical morphology and free AuNP

redistributing back to plasma and excreted in urine [122]. On the other hand, AuNP-liposome nanocomposites coated with PEG have more stable physiochemical properties and pharmacokinetic profile with enhanced permeability and retention (EPR) effect in tumors [193,204], as the half-life was shown in vivo to reach up to 25 hours, staying in the body for up to 14 days [122].

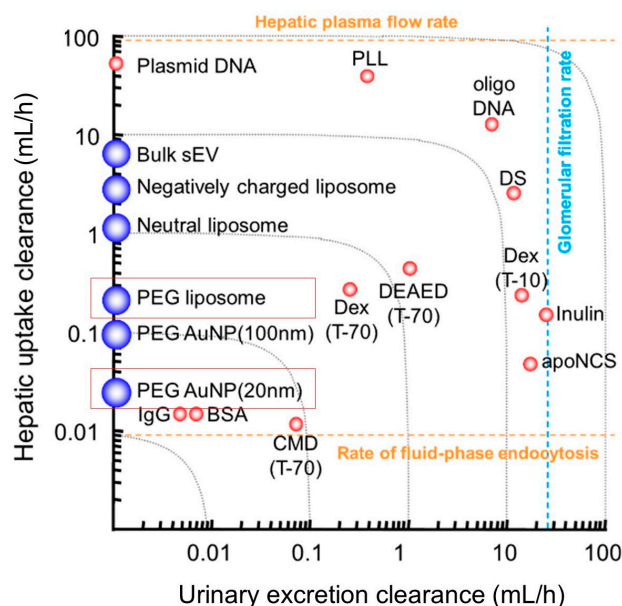


Figure 12. Hepatic uptake and urinary excretion clearances of a variety of macromolecules and nanoparticles in mice after intravenous injection. Nanoparticles include small extracellular vesicles, liposomes, and AuNP [205–209]. AuNP (20 nm) and liposomes (150 nm) are shown in red rectangles. Note: Clearances of nanoparticles are approximate values estimated from the figures shown in the references, since raw data were not available. A direct comparison of data from the same reference is possible. However, attention should be paid when absolute clearance values from different references are compared because experimental designs, such as labeling probes and sampling time schedules, were different. The graph was reproduced with permission from [193], copyright Elsevier 2022.

8. Outlook and Remarks

As discussed above, there are clear driving forces to prepare the AuNP-liposome nanocomposites. Such hybrid nanosystem brings the best of both counterparts: the brilliant optical properties, photothermal effect and imaging modalities for AuNP and the biocompatibility and excellent drug loading of liposomes. The result is a hybrid nanosystem that can be visualized using various imaging platforms, trigger release upon demand with external NIR laser and exhibit superior pharmacokinetics compared to AuNP or liposome alone. The literature is rich of chemical routes to prepare and characterize AuNP-liposome nanocomposites with controlled size, architectures (AuNP special attachment to liposome) and functionality. This topic is still in its early stages and simple synthetic approaches to prepare AuNP-liposome nanocomposites with a capability to be scaled into industrial batches is still to be evaluated and confirmed. Moreover, combining non-biodegradable AuNP into FDA-liposome could bring a regulatory challenge to the composite, especially when the AuNP are larger than being renally cleared as discussed in previous sections. Thus, the chronic safety profile as well as a complete evaluation of the pharmacokinetics of AuNP-liposome nanocomposites should be a subject of upcoming research directions. Overall, from the obtained results in the literature, it is indicated that with further optimization and assessment, AuNP-liposome nanocomposites represent a highly promising approach to fabricate a smart sensing and drug delivery platforms for advanced biomedical and clinical applications in the future.

Author Contributions: Conceptualization, A.M.A.; writing—review and editing, S.I., R.I., A.E., O.R., A.M.A. All authors have read and agreed to the published version of the manuscript.

Funding: This research was funded by Qatar University (Grant number QUT2RP-CPH-23/24-147).

Acknowledgments: Authors acknowledge the financial support from Qatar University.

Conflicts of Interest: The authors declare no conflict of interest.

References

1. Bayda, S.; Adeel, M.; Tuccinardi, T.; Cordani, M.; Rizzolio, F. The History of Nanoscience and Nanotechnology: From Chemical–Physical Applications to Nanomedicine. *Molecules* **2020**, *25*, 112. [[CrossRef](#)]
2. Dreaden, E.C.; Alkilany, A.M.; Huang, X.; Murphy, C.J.; El-Sayed, M.A. The golden age: Gold nanoparticles for biomedicine. *Chem. Soc. Rev.* **2012**, *41*, 2740–2779. [[CrossRef](#)] [[PubMed](#)]
3. Mosleh-Shirazi, S.; Abbasi, M.; Moaddeli, M.R.; Vaez, A.; Shafiee, M.; Kasaei, S.R.; Amani, A.M.; Hatam, S. Nanotechnology Advances in the Detection and Treatment of Cancer: An Overview. *Nanotheranostics* **2022**, *6*, 400–423. [[CrossRef](#)] [[PubMed](#)]
4. Salvador-Morales, C.; Grodzinski, P. Nanotechnology Tools Enabling Biological Discovery. *ACS Nano* **2022**, *16*, 5062–5084. [[CrossRef](#)]
5. Chandra, S.; Hu, T. From Prevention to Therapy: A Roadmap of Nanotechnologies to Stay Ahead of Future Pandemics. *ACS Nano* **2022**, *16*, 9985–9993. [[CrossRef](#)] [[PubMed](#)]
6. Patra, J.K.; Das, G.; Fraceto, L.F.; Campos, E.V.R.; del Pilar Rodriguez-Torres, M.; Acosta-Torres, L.S.; Diaz-Torres, L.A.; Grillo, R.; Swamy, M.K.; Sharma, S.; et al. Nano based drug delivery systems: Recent developments and future prospects. *J. Nanobiotechnol.* **2018**, *16*, 71. [[CrossRef](#)] [[PubMed](#)]
7. Dutta, D.; Das, B.M. Scope of green nanotechnology towards amalgamation of green chemistry for cleaner environment: A review on synthesis and applications of green nanoparticles. *Environ. Nanotechnol. Monit. Manag.* **2020**, *15*, 100418. [[CrossRef](#)]
8. Seaberg, J.; Montazerian, H.; Hossen, M.N.; Bhattacharya, R.; Khademhosseini, A.; Mukherjee, P. Hybrid Nanosystems for Biomedical Applications. *ACS Nano* **2021**, *15*, 2099–2142. [[CrossRef](#)]
9. Meesaragandla, B.; Komaragiri, Y.; Schlüter, R.; Otto, O.; Delcea, M. The impact of cell culture media on the interaction of biopolymer-functionalized gold nanoparticles with cells: Mechanical and toxicological properties. *Sci. Rep.* **2022**, *12*, 16643. [[CrossRef](#)]
10. Bai, X.; Wang, Y.; Song, Z.; Feng, Y.; Chen, Y.; Zhang, D.; Lin, F. The Basic Properties of Gold Nanoparticles and their Applications in Tumor Diagnosis and Treatment. *Int. J. Mol. Sci.* **2020**, *21*, 2480. [[CrossRef](#)]
11. Goddard, Z.R.; Marín, M.J.; Russell, D.A.; Searcey, M. Active targeting of gold nanoparticles as cancer therapeutics. *Chem. Soc. Rev.* **2020**, *49*, 8774–8789. [[CrossRef](#)]
12. Mokammel, M.A.; Islam, M.J.; Hasanuzzaman, M.; Hashmi, S. *Nanoscale Materials for Self-Cleaning and Antibacterial Applications*; Elsevier: Amsterdam, The Netherlands, 2019. [[CrossRef](#)]
13. Huang, X.; El-Sayed, M.A. Gold nanoparticles: Optical properties and implementations in cancer diagnosis and photothermal therapy. *J. Adv. Res.* **2010**, *1*, 13–28. [[CrossRef](#)]
14. Alkilany, A.M.; Lohse, S.E.; Murphy, C.J. The Gold Standard: Gold Nanoparticle Libraries To Understand the Nano–Bio Interface. *Accounts Chem. Res.* **2012**, *46*, 650–661. [[CrossRef](#)] [[PubMed](#)]
15. Carnovale, C.; Bryant, G.; Shukla, R.; Bansal, V. Identifying Trends in Gold Nanoparticle Toxicity and Uptake: Size, Shape, Capping Ligand, and Biological Corona. *ACS Omega* **2019**, *4*, 242–256. [[CrossRef](#)]
16. Stetsenko, M.O.; Rudenko, S.P.; Maksimenko, L.; Serdega, B.K.; Pluchery, O.; Snegir, S.V. Optical Properties of Gold Nanoparticle Assemblies on a Glass Surface. *Nanoscale Res. Lett.* **2017**, *12*, 348. [[CrossRef](#)] [[PubMed](#)]
17. Sulaiman, G.M.; Waheeb, H.M.; Jabir, M.S.; Khazaal, S.H.; Dewir, Y.H.; Naidoo, Y. Hesperidin Loaded on Gold Nanoparticles as a Drug Delivery System for a Successful Biocompatible, Anti-Cancer, Anti-Inflammatory and Phagocytosis Inducer Model. *Sci. Rep.* **2020**, *10*, 9362. [[CrossRef](#)]
18. Jia, Y.-P.; Ma, B.-Y.; Wei, X.-W.; Qian, Z.-Y. The in vitro and in vivo toxicity of gold nanoparticles. *Chin. Chem. Lett.* **2017**, *28*, 691–702. [[CrossRef](#)]
19. Shi, X.; Perry, H.L.; Wilton-Ely, J.D.E.T. Strategies for the functionalisation of gold nanorods to reduce toxicity and aid clinical translation. *Nanotheranostics* **2021**, *5*, 155–165. [[CrossRef](#)] [[PubMed](#)]
20. Eustis, S.; El-Sayed, M.A. Why gold nanoparticles are more precious than pretty gold: Noble metal surface plasmon resonance and its enhancement of the radiative and nonradiative properties of nanocrystals of different shapes. *Chem. Soc. Rev.* **2005**, *35*, 209–217. [[CrossRef](#)]
21. Huang, X.; O'Connor, R.; Kwizera, E.A. Gold Nanoparticle Based Platforms for Circulating Cancer Marker Detection. *Nanotheranostics* **2017**, *1*, 80–102. [[CrossRef](#)]
22. Andreiuk, B.; Nicolson, F.; Clark, L.M.; Panikkanvalappil, S.R.; Rashidian, M.; Harmsen, S.; Kircher, M.F. Design and synthesis of gold nanostars-based SERS nanotags for bioimaging applications. *Nanotheranostics* **2022**, *6*, 10. [[CrossRef](#)] [[PubMed](#)]
23. Grzelczak, M.; Pérez-Juste, J.; Mulvaney, P.; Liz-Marzán, L.M. Shape control in gold nanoparticle synthesis. *Chem. Soc. Rev.* **2008**, *37*, 1783–1791. [[CrossRef](#)]

24. Rahmati, S.; Doherty, W.; Babadi, A.A.; Mansor, M.A.C.; Julkapli, N.; Hessel, V.; Ostrikov, K. Gold–Carbon Nanocomposites for Environmental Contaminant Sensing. *Micromachines* **2021**, *12*, 719. [[CrossRef](#)] [[PubMed](#)]
25. Shi, P.; Xue, R.; Wei, Y.; Lei, X.; Ai, J.; Wang, T.; Shi, Z.; Wang, X.; Wang, Q.; Soliman, F.M.; et al. Gold nanoparticles/tetraaminophenyl porphyrin functionalized multiwalled carbon nanotubes nanocomposites modified glassy carbon electrode for the simultaneous determination of p-acetaminophen and p-aminophenol. *Arab. J. Chem.* **2020**, *13*, 1040–1051. [[CrossRef](#)]
26. Kim, G.H.; Kim, K.; Nam, H.; Shin, K.; Choi, W.; Shin, J.H.; Lim, G. CNT-Au nanocomposite deposition on gold microelectrodes for improved neural recordings. *Sens. Actuators B Chem.* **2017**, *252*, 152–158. [[CrossRef](#)]
27. Zhang, R.-C.; Sun, D.; Zhang, R.; Lin, W.-F.; Macias-Montero, M.; Patel, J.; Askari, S.; McDonald, C.; Mariotti, D.; Maguire, P. Gold nanoparticle-polymer nanocomposites synthesized by room temperature atmospheric pressure plasma and their potential for fuel cell electrocatalytic application. *Sci. Rep.* **2017**, *7*, 46682. [[CrossRef](#)]
28. Afzali, M.; Mostafavi, A.; Shamspur, T. Developing a novel sensor based on ionic liquid molecularly imprinted polymer/gold nanoparticles/graphene oxide for the selective determination of an anti-cancer drug imiquimod. *Biosens. Bioelectron.* **2019**, *143*, 111620. [[CrossRef](#)]
29. Yu, Y.; Si, J.; Yan, L.; Li, M.; Hou, X. Enhanced nonlinear absorption and ultrafast carrier dynamics in graphene/gold nanoparticles nanocomposites. *Carbon* **2019**, *148*, 72–79. [[CrossRef](#)]
30. Zhang, C.; Zhang, Y.; Miao, Z.; Ma, M.; Du, X.; Lin, J.; Han, B.; Takahashi, S.; Anzai, J.-I.; Chen, Q. Dual-function amperometric sensors based on poly(diallyldimethylammonium chloride)-functionalized reduced graphene oxide/manganese dioxide/gold nanoparticles nanocomposite. *Sens. Actuators B Chem.* **2016**, *222*, 663–673. [[CrossRef](#)]
31. Bolaños, K.; Kogan, M.J.; Araya, E. Capping gold nanoparticles with albumin to improve their biomedical properties. *Int. J. Nanomed.* **2019**, *14*, 6387–6406. [[CrossRef](#)]
32. Li, T.; Wang, Y.; Wang, M.; Zheng, L.; Dai, W.; Jiao, C.; Song, Z.; Ma, Y.; Ding, Y.; Zhang, Z.; et al. Impact of Albumin Pre-Coating on Gold Nanoparticles Uptake at Single-Cell Level. *Nanomaterials* **2022**, *12*, 749. [[CrossRef](#)] [[PubMed](#)]
33. Sanzhakov, M.; Kudinov, V.; Baskaev, K.; Morozovich, G.; Stepanova, D.; Torkhovskaya, T.; Tereshkina, Y.A.; Korotkevich, E.; Tikhonova, E. Composite phospholipid-gold nanoparticles with targeted fragment for tumor imaging. *Biomed. Pharmacother.* **2021**, *142*, 111985. [[CrossRef](#)]
34. Pornpattananangkul, D.; Zhang, L.; Olson, S.; Aryal, S.; Obonyo, M.; Vecchio, K.; Huang, C.-M.; Zhang, L. Bacterial Toxin-Triggered Drug Release from Gold Nanoparticle-Stabilized Liposomes for the Treatment of Bacterial Infection. *J. Am. Chem. Soc.* **2011**, *133*, 4132–4139. [[CrossRef](#)] [[PubMed](#)]
35. Alkilany, A.M.; Rachid, O.; Alkawareek, M.Y.; Billa, N.; Daou, A.; Murphy, C.J. PLGA-Gold Nanocomposite: Preparation and Biomedical Applications. *Pharmaceutics* **2022**, *14*, 660. [[CrossRef](#)]
36. Alkilany, A.M.; Abulateefeh, S.R.; Murphy, C.J. Facile Functionalization of Gold Nanoparticles with PLGA Polymer Brushes and Efficient Encapsulation into PLGA Nanoparticles: Toward Spatially Precise Bioimaging of Polymeric Nanoparticles. *Part. Part. Syst. Charact.* **2018**, *36*, 1800414. [[CrossRef](#)]
37. Veeren, A.; Ogunyankin, M.O.; Shin, J.E.; Zasadzinski, J.A. Liposome-Tethered Gold Nanoparticles Triggered by Pulsed NIR Light for Rapid Liposome Contents Release and Endosome Escape. *Pharmaceutics* **2022**, *14*, 701. [[CrossRef](#)] [[PubMed](#)]
38. Wu, G.; Mikhailovsky, A.; Khant, H.A.; Zasadzinski, J.A. Synthesis, Characterization, and Optical Response of Gold Nanoshells Used to Trigger Release from Liposomes. *Methods Enzymol.* **2009**, *464*, 279–307. [[CrossRef](#)]
39. Kojima, C.; Hirano, Y.; Kono, K. Preparation of Complexes of Liposomes with Gold Nanoparticles. *Methods Enzymol.* **2009**, *464*, 131–145. [[CrossRef](#)]
40. Edwards, P.P.; Thomas, J.M. Gold in a Metallic Divided State—From Faraday to Present-Day Nanoscience. *Angew. Chem. Int. Ed.* **2007**, *46*, 5480–5486. [[CrossRef](#)]
41. Dieringer, J.A.; McFarland, A.M.; Shah, N.C.; Stuart, D.A.; Whitney, A.V.; Yonzon, C.R.; Young, M.A.; Zhang, X.; Duyne, R.P.V. Introductory Lecture: Surface enhanced Raman spectroscopy: New materials, concepts, characterization tools, and applications. *Faraday Discuss.* **2006**, *132*. [[CrossRef](#)]
42. Rastinehad, A.R.; Anastos, H.; Wajswol, E.; Winoker, J.S.; Sfakianos, J.P.; Doppalapudi, S.K.; Carrick, M.R.; Knauer, C.J.; Taouli, B.; Lewis, S.C.; et al. Gold nanoshell-localized photothermal ablation of prostate tumors in a clinical pilot device study. *Proc. Natl. Acad. Sci. USA* **2019**, *116*, 18590–18596. [[CrossRef](#)]
43. Amina, S.J.; Guo, B. A Review on the Synthesis and Functionalization of Gold Nanoparticles as a Drug Delivery Vehicle. *Int. J. Nanomed.* **2020**, *15*, 9823–9857. [[CrossRef](#)]
44. Amendola, V.; Polizzi, S.; Meneghetti, M. Laser Ablation Synthesis of Gold Nanoparticles in Organic Solvents. *J. Phys. Chem. B* **2006**, *110*, 7232–7237. [[CrossRef](#)]
45. Raliya, R.; Saha, D.; Chadha, T.S.; Raman, B.; Biswas, P. Non-invasive aerosol delivery and transport of gold nanoparticles to the brain. *Sci. Rep.* **2017**, *7*, srep44718. [[CrossRef](#)]
46. Hainfeld, J.F.; O'Connor, M.J.; Lin, P.; Qian, L.; Slatkin, D.N.; Smilowitz, H.M. Infrared-Transparent Gold Nanoparticles Converted by Tumors to Infrared Absorbers Cure Tumors in Mice by Photothermal Therapy. *PLoS ONE* **2014**, *9*, e88414. [[CrossRef](#)]
47. Hatakeyama, Y.; Onishi, K.; Nishikawa, K. Effects of sputtering conditions on formation of gold nanoparticles in sputter deposition technique. *RSC Adv.* **2011**, *1*, 1815–1821. [[CrossRef](#)]

48. Hühn, J.; Carrillo-Carrion, C.; Soliman, M.G.; Pfeiffer, C.; Valdeperez, D.; Masood, A.; Chakraborty, I.; Zhu, L.; Gallego, M.; Yue, Z.; et al. Selected Standard Protocols for the Synthesis, Phase Transfer, and Characterization of Inorganic Colloidal Nanoparticles. *Chem. Mater.* **2016**, *29*, 399–461. [[CrossRef](#)]
49. Xia, H.; Xiahou, Y.; Zhang, P.; Ding, W.; Wang, D. Revitalizing the Frens Method To Synthesize Uniform, Quasi-Spherical Gold Nanoparticles with Deliberately Regulated Sizes from 2 to 330 nm. *Langmuir* **2016**, *32*, 5870–5880. [[CrossRef](#)] [[PubMed](#)]
50. Frens, G. Controlled Nucleation for the Regulation of the Particle Size in Monodisperse Gold Suspensions. *Nat. Phys. Sci.* **1973**, *241*, 20–22. [[CrossRef](#)]
51. Brust, M.; Walker, M.; Bethell, D.; Schiffrin, D.J.; Whyman, R. Synthesis of thiol-derivatised gold nanoparticles in a two-phase Liquid–Liquid system. *J. Chem. Soc. Chem. Commun.* **1994**, *1994*, 801–802. [[CrossRef](#)]
52. Sánchez-Iglesias, A.; Winckelmans, N.; Altantzis, T.; Bals, S.; Grzelczak, M.; Liz-Marzán, L.M. High-Yield Seeded Growth of Monodisperse Pentatwinned Gold Nanoparticles through Thermally Induced Seed Twinning. *J. Am. Chem. Soc.* **2016**, *139*, 107–110. [[CrossRef](#)] [[PubMed](#)]
53. Nikoobakht, B.; El-Sayed, M.A. Preparation and Growth Mechanism of Gold Nanorods (NRs) Using Seed-Mediated Growth Method. *Chem. Mater.* **2003**, *15*, 1957–1962. [[CrossRef](#)]
54. Chang, H.-H.; Murphy, C.J. Mini Gold Nanorods with Tunable Plasmonic Peaks beyond 1000 nm. *Chem. Mater.* **2018**, *30*, 1427–1435. [[CrossRef](#)]
55. Ye, X.; Gao, Y.; Chen, J.; Reifsnnyder, D.C.; Zheng, C.; Murray, C.B. Seeded Growth of Monodisperse Gold Nanorods Using Bromide-Free Surfactant Mixtures. *Nano Lett.* **2013**, *13*, 2163–2171. [[CrossRef](#)]
56. Sun, Y.; Xia, Y. Shape-Controlled Synthesis of Gold and Silver Nanoparticles. *Science* **2002**, *298*, 2176–2179. [[CrossRef](#)]
57. Li, C.; Shuford, K.L.; Chen, M.; Lee, E.J.; Cho, S.O. A Facile Polyol Route to Uniform Gold Octahedra with Tailorable Size and Their Optical Properties. *ACS Nano* **2008**, *2*, 1760–1769. [[CrossRef](#)]
58. Lee, K.X.; Shameli, K.; Miyake, M.; Kuwano, N.; Khairudin, N.B.B.A.; Mohamad, S.E.B.; Yew, Y.P. Green Synthesis of Gold Nanoparticles Using Aqueous Extract of *Garcinia mangostana* Fruit Peels. *J. Nanomater.* **2016**, *2016*, 8489094. [[CrossRef](#)]
59. Ramakrishna, M.; Babu, D.R.; Gengan, R.M.; Chandra, S.; Rao, G.N. Green synthesis of gold nanoparticles using marine algae and evaluation of their catalytic activity. *J. Nanostruct. Chem.* **2015**, *6*, 77–82. [[CrossRef](#)]
60. Iranmanesh, S.; Bonjar, G.H.S.; Baghizadeh, A. Study of the biosynthesis of gold nanoparticles by using several saprophytic fungi. *SN Appl. Sci.* **2020**, *2*, 1851. [[CrossRef](#)]
61. He, S.; Guo, Z.; Zhang, Y.; Zhang, S.; Wang, J.; Gu, N. Biosynthesis of gold nanoparticles using the bacteria *Rhodospseudomonas capsulata*. *Mater. Lett.* **2007**, *61*, 3984–3987. [[CrossRef](#)]
62. Bansal, S.A.; Kumar, V.; Karimi, J.; Singh, A.P.; Kumar, S. Role of gold nanoparticles in advanced biomedical applications. *Nanoscale Adv.* **2020**, *2*, 3764–3787. [[CrossRef](#)] [[PubMed](#)]
63. Milan, J.; Niemczyk, K.; Kus-Liśkiewicz, M. Treasure on the Earth—Gold Nanoparticles and Their Biomedical Applications. *Materials* **2022**, *15*, 3355. [[CrossRef](#)] [[PubMed](#)]
64. Chuang, Y.-C.; Lee, H.-L.; Chiou, J.-F.; Lo, L.-W. Recent Advances in Gold Nanomaterials for Photothermal Therapy. *J. Nanotheranostics* **2022**, *3*, 117–131. [[CrossRef](#)]
65. Kumar, A.; Das, N.; Rayavarapu, R.G. Role of Tunable Gold Nanostructures in Cancer Nanotheranostics: Implications on Synthesis, Toxicity, Clinical Applications and Their Associated Opportunities and Challenges. *J. Nanotheranostics* **2023**, *4*, 1–34. [[CrossRef](#)]
66. Ferrari, E. Gold Nanoparticle-Based Plasmonic Biosensors. *Biosensors* **2023**, *13*, 411. [[CrossRef](#)]
67. Chang, C.-C.; Chen, C.-P.; Wu, T.-H.; Yang, C.-H.; Lin, C.-W.; Chen, C.-Y. Gold Nanoparticle-Based Colorimetric Strategies for Chemical and Biological Sensing Applications. *Nanomaterials* **2019**, *9*, 861. [[CrossRef](#)]
68. Kumar, D.; Saini, N.; Jain, N.; Sareen, R.; Pandit, V. Gold nanoparticles: An era in bionanotechnology. *Expert Opin. Drug Deliv.* **2013**, *10*, 397–409. [[CrossRef](#)]
69. Weigel, A.; Sebesta, A.; Kukura, P. Dark Field Microspectroscopy with Single Molecule Fluorescence Sensitivity. *ACS Photonics* **2014**, *1*, 848–856. [[CrossRef](#)]
70. Boby, N.; Ali, S.A.; Preena, P.; Kaur, G.; Kumar, S.; Chaudhuri, P. Detection of multiple organisms based on the distance-dependent optical properties of gold nanoparticle and dark-field microscopy. *Talanta* **2018**, *188*, 325–331. [[CrossRef](#)]
71. D’Acunto, M. Detection of Intracellular Gold Nanoparticles: An Overview. *Materials* **2018**, *11*, 882. [[CrossRef](#)]
72. SoRelle, E.D.; Liba, O.; Campbell, J.L.; Dalal, R.; Zavaleta, C.L.; de la Zerda, A. A hyperspectral method to assay the microphysiological fates of nanomaterials in histological samples. *Elife* **2016**, *5*, e16352. [[CrossRef](#)] [[PubMed](#)]
73. Aldosari, F.M.M. Characterization of Labeled Gold Nanoparticles for Surface-Enhanced Raman Scattering. *Molecules* **2022**, *27*, 892. [[CrossRef](#)]
74. Wu, X.; Peng, Y.; Duan, X.; Yang, L.; Lan, J.; Wang, F. Homologous Gold Nanoparticles and Nanoclusters Composites with Enhanced Surface Raman Scattering and Metal Fluorescence for Cancer Imaging. *Nanomaterials* **2018**, *8*, 819. [[CrossRef](#)] [[PubMed](#)]
75. Zhang, Z.; Yang, P.; Xu, H.; Zheng, H. Surface enhanced fluorescence and Raman scattering by gold nanoparticle dimers and trimers. *J. Appl. Phys.* **2013**, *113*, 033102. [[CrossRef](#)]
76. Cao, Y.; Qian, R.-C.; Li, D.-W.; Long, Y.-T. Raman/fluorescence dual-sensing and imaging of intracellular pH distribution. *Chem. Commun.* **2015**, *51*, 17584–17587. [[CrossRef](#)] [[PubMed](#)]

77. Iosin, M.; Toderas, F.; Baldeck, P.; Astilean, S. Study of protein–gold nanoparticle conjugates by fluorescence and surface-enhanced Raman scattering. *J. Mol. Struct.* **2009**, *924–926*, 196–200. [[CrossRef](#)]
78. Venditti, I.; Cartoni, A.; Cerra, S.; Fioravanti, R.; Salamone, T.A.; Sciubba, F.; Tabocchini, M.A.; Dini, V.; Battocchio, C.; Iucci, G.; et al. Hydrophilic Gold Nanoparticles as Anti-PD-L1 Antibody Carriers: Synthesis and Interface Properties. *Part. Part. Syst. Charact.* **2022**, *39*, 2100282. [[CrossRef](#)]
79. El-Sayed, I.H.; Huang, X.; El-Sayed, M.A. Selective laser photo-thermal therapy of epithelial carcinoma using anti-EGFR antibody conjugated gold nanoparticles. *Cancer Lett.* **2006**, *239*, 129–135. [[CrossRef](#)]
80. Huang, X.; El-Sayed, I.H.; Qian, W.; El-Sayed, M.A. Cancer Cell Imaging and Photothermal Therapy in the Near-Infrared Region by Using Gold Nanorods. *J. Am. Chem. Soc.* **2006**, *128*, 2115–2120. [[CrossRef](#)]
81. Hirsch, L.R.; Stafford, R.J.; Bankson, J.A.; Sershen, S.R.; Rivera, B.; Price, R.E.; Hazle, J.D.; Halas, N.J.; West, J.L. Nanoshell-mediated near-infrared thermal therapy of tumors under magnetic resonance guidance. *Proc. Natl. Acad. Sci. USA* **2003**, *100*, 13549–13554. [[CrossRef](#)]
82. Rodzik-Czałka, Ł.; Lewandowska-Łańcucka, J.; Gatta, V.; Venditti, I.; Fratoddi, I.; Szuwarzyński, M.; Romek, M.; Nowakowska, M. Nucleobases functionalized quantum dots and gold nanoparticles bioconjugates as a fluorescence resonance energy transfer (FRET) system—Synthesis, characterization and potential applications. *J. Colloid Interface Sci.* **2017**, *514*, 479–490. [[CrossRef](#)]
83. Yang, W.; Liang, H.; Ma, S.; Wang, D.; Huang, J. Gold nanoparticle based photothermal therapy: Development and application for effective cancer treatment. *Sustain. Mater. Technol.* **2019**, *22*, e00109. [[CrossRef](#)]
84. Sun, M.; Liu, F.; Zhu, Y.; Wang, W.; Hu, J.; Liu, J.; Dai, Z.; Wang, K.; Wei, Y.; Bai, J.; et al. Salt-induced aggregation of gold nanoparticles for photoacoustic imaging and photothermal therapy of cancer. *Nanoscale* **2016**, *8*, 4452–4457. [[CrossRef](#)] [[PubMed](#)]
85. Kim, H.S.; Lee, D.Y. Near-Infrared-Responsive Cancer Photothermal and Photodynamic Therapy Using Gold Nanoparticles. *Polymers* **2018**, *10*, 961. [[CrossRef](#)]
86. Sun, M.; Peng, D.; Hao, H.; Hu, J.; Wang, D.; Wang, K.; Liu, J.; Guo, X.; Wei, Y.; Gao, W. Thermally Triggered in Situ Assembly of Gold Nanoparticles for Cancer Multimodal Imaging and Photothermal Therapy. *ACS Appl. Mater. Interfaces* **2017**, *9*, 10453–10460. [[CrossRef](#)]
87. Ali, M.R.K.; Wu, Y.; El-Sayed, M.A. Gold-Nanoparticle-Assisted Plasmonic Photothermal Therapy Advances Toward Clinical Application. *J. Phys. Chem. C* **2019**, *123*, 15375–15393. [[CrossRef](#)]
88. Manrique-Bedoya, S.; Abdul-Moqueet, M.; Lopez, P.; Gray, T.; Disiena, M.; Locker, A.; Kwee, S.; Tang, L.; Hood, R.L.; Feng, Y.; et al. Multiphysics Modeling of Plasmonic Photothermal Heating Effects in Gold Nanoparticles and Nanoparticle Arrays. *J. Phys. Chem. C* **2020**, *124*, 17172–17182. [[CrossRef](#)] [[PubMed](#)]
89. Yang, Z.; Wang, D.; Zhang, C.; Liu, H.; Hao, M.; Kan, S.; Liu, D.; Liu, W. The Applications of Gold Nanoparticles in the Diagnosis and Treatment of Gastrointestinal Cancer. *Front. Oncol.* **2022**, *11*, 819329. [[CrossRef](#)]
90. Maurizi, L.; Forte, J.; Ammendolia, M.G.; Hanieh, P.N.; Conte, A.L.; Relucenti, M.; Donfrancesco, O.; Ricci, C.; Rinaldi, F.; Marianecchi, C.; et al. Effect of Ciprofloxacin-Loaded Niosomes on *Escherichia coli* and *Staphylococcus aureus* Biofilm Formation. *Pharmaceutics* **2022**, *14*, 2662. [[CrossRef](#)]
91. Musielak, E.; Feliczak-Guzik, A.; Nowak, I. Synthesis and Potential Applications of Lipid Nanoparticles in Medicine. *Materials* **2022**, *15*, 682. [[CrossRef](#)]
92. Bangham, A.D.; Hill, M.W.; Miller, N.G.A. Preparation and Use of Liposomes as Models of Biological Membranes. In *Methods in Membrane Biology*; Springer: Boston, MA, USA, 1974; pp. 1–68. [[CrossRef](#)]
93. Bozzuto, G.; Molinari, A. Liposomes as nanomedical devices. *Int. J. Nanomed.* **2015**, *10*, 975–999. [[CrossRef](#)]
94. Lombardo, D.; Kiselev, M.A. Methods of Liposomes Preparation: Formation and Control Factors of Versatile Nanocarriers for Biomedical and Nanomedicine Application. *Pharmaceutics* **2022**, *14*, 543. [[CrossRef](#)]
95. Šturm, L.; Ulrih, N.P. Basic Methods for Preparation of Liposomes and Studying Their Interactions with Different Compounds, with the Emphasis on Polyphenols. *Int. J. Mol. Sci.* **2021**, *22*, 6547. [[CrossRef](#)]
96. Dua, J.S.; Rana, A.C.; Bhandari, A.K. Liposome: Methods of preparation and applications. *Int. J. Pharm. Stud. Res.* **2012**, *3*, 14–20.
97. William, B.; Noémie, P.; Brigitte, E.; Géraldine, P. Supercritical fluid methods: An alternative to conventional methods to prepare liposomes. *Chem. Eng. J.* **2020**, *383*, 123106. [[CrossRef](#)]
98. Van Rooijen, N.; Sanders, A. Liposome mediated depletion of macrophages: Mechanism of action, preparation of liposomes and applications. *J. Immunol. Methods* **1994**, *174*, 83–93. [[CrossRef](#)]
99. Xu, L.; Wang, X.; Liu, Y.; Yang, G.; Falconer, R.J.; Zhao, C.-X. Lipid Nanoparticles for Drug Delivery. *Adv. NanoBiomed Res.* **2021**, *2*, 2100109. [[CrossRef](#)]
100. Cunha, S.; Amaral, M.H.; Lobo, J.M.S.; Silva, A.C. Lipid Nanoparticles for Nasal/Intranasal Drug Delivery. *Crit. Rev. Ther. Drug Carr. Syst.* **2017**, *34*, 257–282. [[CrossRef](#)] [[PubMed](#)]
101. Mirchandani, Y.; Patravale, V.B.; Brijesh, S. Solid lipid nanoparticles for hydrophilic drugs. *J. Control Release* **2021**, *335*, 457–464. [[CrossRef](#)] [[PubMed](#)]
102. da Silva, G.H.R.; de Moura, L.D.; de Carvalho, F.V.; Geronimo, G.; Mendonça, T.C.; de Lima, F.F.; de Paula, E. Antineoplastics Encapsulated in Nanostructured Lipid Carriers. *Molecules* **2021**, *26*, 6929. [[CrossRef](#)]
103. Al Saqr, A.; Wani, S.U.D.; Gangadharappa, H.V.; Aldawsari, M.F.; Khafagy, E.-S.; Abu Lila, A.S. Enhanced Cytotoxic Activity of Docetaxel-Loaded Silk Fibroin Nanoparticles against Breast Cancer Cells. *Polymers* **2021**, *13*, 1416. [[CrossRef](#)] [[PubMed](#)]

104. Ren, G.; Liu, D.; Guo, W.; Wang, M.; Wu, C.; Guo, M.; Ai, X.; Wang, Y.; He, Z. Docetaxel prodrug liposomes for tumor therapy: Characterization, in vitro and in vivo evaluation. *Drug Deliv.* **2016**, *23*, 1272–1281. [[CrossRef](#)]
105. Batist, G.; Barton, J.; Chaikin, P.; Swenson, C.; Welles, L. Myocet (liposome-encapsulated doxorubicin citrate): A new approach in breast cancer therapy. *Expert Opin. Pharmacother.* **2002**, *3*, 1739–1751. [[CrossRef](#)] [[PubMed](#)]
106. Bulbake, U.; Doppalapudi, S.; Kommineni, N.; Khan, W. Liposomal Formulations in Clinical Use: An Updated Review. *Pharmaceutics* **2017**, *9*, 12. [[CrossRef](#)]
107. Adler-Moore, J.; Proffitt, R.T. AmBisome: Liposomal formulation, structure, mechanism of action and pre-clinical experience. *J. Antimicrob. Chemother.* **2002**, *49*, 21–30. [[CrossRef](#)]
108. Barenholz, Y. Doxil[®]—The first FDA-approved nano-drug: Lessons learned. *J. Control Release* **2012**, *160*, 117–134. [[CrossRef](#)]
109. Liu, P.; Chen, G.; Zhang, J. A Review of Liposomes as a Drug Delivery System: Current Status of Approved Products, Regulatory Environments, and Future Perspectives. *Molecules* **2022**, *27*, 1372. [[CrossRef](#)] [[PubMed](#)]
110. Ahmed, K.S.; Liu, S.; Mao, J.; Zhang, J.; Qiu, L. Dual-Functional Peptide Driven Liposome Codelivery System for Efficient Treatment of Doxorubicin-Resistant Breast Cancer. *Drug Des. Dev. Ther.* **2021**, *15*, 3223–3239. [[CrossRef](#)]
111. He, Q.; He, X.; Deng, B.; Shi, C.; Lin, L.; Liu, P.; Yang, Z.; Yang, S.; Xu, Z. Sorafenib and indocyanine green co-loaded in photothermally sensitive liposomes for diagnosis and treatment of advanced Hepatocellular carcinoma Qianyuan. *J. Mater. Chem. B* **2018**, *6*, 5823–5834. [[CrossRef](#)]
112. Cheng, M.H.Y.; Harmatys, K.M.; Charron, D.M.; Chen, J.; Zheng, G. Stable J-Aggregation of an aza-BODIPY-Lipid in a Liposome for Optical Cancer Imaging. *Angew. Chem.* **2019**, *131*, 13528–13533. [[CrossRef](#)]
113. Ren, H.; He, Y.; Liang, J.; Cheng, Z.; Zhang, M.; Zhu, Y.; Hong, C.; Qin, J.; Xu, X.; Wang, J. Role of Liposome Size, Surface Charge, and PEGylation on Rheumatoid Arthritis Targeting Therapy. *ACS Appl. Mater. Interfaces* **2019**, *11*, 20304–20315. [[CrossRef](#)]
114. Ganesan, P.; Narayanasamy, D. Lipid nanoparticles: Different preparation techniques, characterization, hurdles, and strategies for the production of solid lipid nanoparticles and nanostructured lipid carriers for oral drug delivery. *Sustain. Chem. Pharm.* **2017**, *6*, 37–56. [[CrossRef](#)]
115. Vargas, K.M.; Shon, Y.-S. Hybrid lipid–nanoparticle complexes for biomedical applications. *J. Mater. Chem. B* **2019**, *7*, 695–708. [[CrossRef](#)] [[PubMed](#)]
116. Thostenson, E.; Li, C.; Chou, T. Nanocomposites in context. *Compos. Sci. Technol.* **2005**, *65*, 491–516. [[CrossRef](#)]
117. Das, D.; Kar, T.; Das, P.K. Gel-nanocomposites: Materials with promising applications. *Soft Matter* **2011**, *8*, 2348–2365. [[CrossRef](#)]
118. Elgohary, M.M.; Helmy, M.W.; Mortada, S.M.; Elzoghby, A.O. Dual-targeted nano-in-nano albumin carriers enhance the efficacy of combined chemo / herbal therapy of lung cancer. *Nanomedicine* **2018**, *13*, 2221–2224. [[CrossRef](#)] [[PubMed](#)]
119. Zhao, Z.; Lou, S.; Hu, Y.; Zhu, J.; Zhang, C. A Nano-in-Nano Polymer–Dendrimer Nanoparticle-Based Nanosystem for Controlled Multidrug Delivery. *Mol. Pharm.* **2017**, *14*, 2697–2710. [[CrossRef](#)]
120. Dichello, G.A.; Fukuda, T.; Maekawa, T.; Whitby, R.L.; Mikhalovsky, S.V.; Alavijeh, M.; Pannala, A.S.; Sarker, D.K. Preparation of liposomes containing small gold nanoparticles using electrostatic interactions. *Eur. J. Pharm. Sci.* **2017**, *105*, 55–63. [[CrossRef](#)]
121. Pornpattananangkul, D.; Olson, S.; Aryal, S.; Sartor, M.; Huang, C.-M.; Vecchio, K.; Zhang, L. Stimuli-Responsive Liposome Fusion Mediated by Gold Nanoparticles. *ACS Nano* **2010**, *4*, 1935–1942. [[CrossRef](#)]
122. Rengan, A.K.; Bukhari, A.B.; Pradhan, A.; Malhotra, R.; Banerjee, R.; Srivastava, R.; De, A. In Vivo Analysis of Biodegradable Liposome Gold Nanoparticles as Efficient Agents for Photothermal Therapy of Cancer. *Nano Lett.* **2015**, *15*, 842–848. [[CrossRef](#)]
123. Mathiyazhakan, M.; Wiraja, C.; Xu, C. A Concise Review of Gold Nanoparticles-Based Photo-Responsive Liposomes for Controlled Drug Delivery. *Nano-Micro Lett.* **2017**, *10*, 10. [[CrossRef](#)] [[PubMed](#)]
124. Musielak, M.; Potoczny, J.; Boś-Liedke, A.; Kozak, M. The Combination of Liposomes and Metallic Nanoparticles as Multifunctional Nanostructures in the Therapy and Medical Imaging—A Review. *Int. J. Mol. Sci.* **2021**, *22*, 6229. [[CrossRef](#)]
125. Arvizo, R.; Bhattacharya, R.; Mukherjee, P. Gold nanoparticles: Opportunities and challenges in nanomedicine. *Expert Opin. Drug Deliv.* **2010**, *7*, 753–763. [[CrossRef](#)]
126. Taguchi, K.; Okamoto, Y.; Matsumoto, K.; Otagiri, M.; Chuang, V.T.G. When Albumin Meets Liposomes: A Feasible Drug Carrier for Biomedical Applications. *Pharmaceutics* **2021**, *14*, 296. [[CrossRef](#)]
127. Seo, M.-W.; Park, T.-E. Recent advances with liposomes as drug carriers for treatment of neurodegenerative diseases. *Biomed. Eng. Lett.* **2021**, *11*, 211–216. [[CrossRef](#)] [[PubMed](#)]
128. Adler-Moore, J.P.; Proffitt, R.T. Development, Characterization, Efficacy and Mode of Action of Ambisome, A Unilamellar Liposomal Formulation of Amphotericin B. *J. Liposome Res.* **1993**, *3*, 429–450. [[CrossRef](#)]
129. Hong, K.; Friend, D.S.; Glabe, C.G.; Papahadjopoulos, D. Liposomes containing colloidal gold are a useful probe of liposome-cell interactions. *Biochim. Biophys. Acta* **1983**, *732*, 320–323. [[CrossRef](#)]
130. Singh, S.P.; Alvi, S.B.; Pemmaraju, D.B.; Singh, A.D.; Manda, S.V.; Srivastava, R.; Rengan, A.K. NIR triggered liposome gold nanoparticles entrapping curcumin as in situ adjuvant for photothermal treatment of skin cancer. *Int. J. Biol. Macromol.* **2018**, *110*, 375–382. [[CrossRef](#)]
131. Chauhan, D.S.; Prasad, R.; Devrukhkar, J.; Selvaraj, K.; Srivastava, R. Disintegrable NIR Light Triggered Gold Nanorods Supported Liposomal Nanohybrids for Cancer Theranostics. *Bioconj. Chem.* **2017**, *29*, 1510–1518. [[CrossRef](#)] [[PubMed](#)]
132. Zhang, Y.; Hao, S.; Zuo, J.; Guo, H.; Liu, M.; Zhu, H.; Sun, H. NIR-Activated Thermosensitive Liposome–Gold Nanorod Hybrids for Enhanced Drug Delivery and Stimulus Sensitivity. *ACS Biomater. Sci. Eng.* **2022**, *9*, 340–351. [[CrossRef](#)]

133. Goh, E.T.H.; Cheung, P.C.F.; Akira, S.; Centre, B.; Defense, H. Doxorubicin/gold nanoparticles coated with liposomes for chemophotothermal synergetic antitumor therapy. *Nanotechnology* **2018**, *29*, 405101.
134. Luchini, A.; D'errico, G.; Leone, S.; Vaezi, Z.; Bortolotti, A.; Stella, L.; Vitiello, G.; Paduano, L. Structural organization of lipid-functionalized-Au nanoparticles. *Colloids Surf. B Biointerfaces* **2018**, *168*, 2–9. [[CrossRef](#)]
135. Tao, Y.; Han, J.; Ye, C.; Thomas, T.; Dou, H. Reduction-responsive gold-nanoparticle-conjugated Pluronic micelles: An effective anti-cancer drug delivery system. *J. Mater. Chem.* **2012**, *22*, 18864–18871. [[CrossRef](#)]
136. Zhang, L.; Granick, S. How to Stabilize Phospholipid Liposomes (Using Nanoparticles). *Nano Lett.* **2006**, *6*, 694–698. [[CrossRef](#)] [[PubMed](#)]
137. Sugikawa, K.; Matsuo, K.; Ikeda, A. Suppression of Gold Nanoparticle Aggregation on Lipid Membranes Using Nanosized Liposomes To Increase Steric Hindrance. *Langmuir* **2018**, *35*, 229–236. [[CrossRef](#)] [[PubMed](#)]
138. Takahashi, H.; Niidome, Y.; Niidome, T.; Kaneko, K.; Kawasaki, H.; Yamada, S. Modification of Gold Nanorods Using Phosphatidylcholine to Reduce Cytotoxicity. *Langmuir* **2005**, *22*, 2–5. [[CrossRef](#)]
139. Lee, J.-H.; Shin, Y.; Lee, W.; Whang, K.; Kim, D.; Lee, L.P.; Choi, J.-W.; Kang, T. General and programmable synthesis of hybrid liposome/metal nanoparticles. *Sci. Adv.* **2016**, *2*, e1601838. [[CrossRef](#)]
140. Barroso, M.F.; Luna, M.A.; Tabares, J.S.F.; Delerue-Matos, C.; Correa, N.M.; Moyano, F.; Molina, P.G. Gold nanoparticles covalently assembled onto vesicle structures as possible biosensing platform. *Beilstein J. Nanotechnol.* **2016**, *7*, 655–663. [[CrossRef](#)]
141. Paasonen, L.; Sipilä, T.; Subrizi, A.; Laurinmäki, P.; Butcher, S.J.; Rappolt, M.; Yagmur, A.; Urtti, A.; Yliperttula, M. Gold-embedded photosensitive liposomes for drug delivery: Triggering mechanism and intracellular release. *J. Control Release* **2010**, *147*, 136–143. [[CrossRef](#)]
142. Park, S.-H.; Oh, S.-G.; Mun, J.-Y.; Han, S.-S. Loading of gold nanoparticles inside the DPPC bilayers of liposome and their effects on membrane fluidities. *Colloids Surf. B Biointerfaces* **2006**, *48*, 112–118. [[CrossRef](#)]
143. Regan, D.; Williams, J.B.; Borri, P.; Langbein, W. Lipid Bilayer Thickness Measured by Quantitative DIC Reveals Phase Transitions and Effects of Substrate Hydrophilicity. *Langmuir* **2019**, *35*, 13805–13814. [[CrossRef](#)] [[PubMed](#)]
144. Szoka, F.; Papahadjopoulos, D. Comparative Properties and Methods of Preparation of Lipid Vesicles (Liposomes). *Annu. Rev. Biophys. Bioeng.* **1980**, *9*, 467–508. [[CrossRef](#)] [[PubMed](#)]
145. Olson, F.; Hunt, C.; Szoka, F.; Vail, W.; Papahadjopoulos, D. Preparation of liposomes of defined size distribution by extrusion through polycarbonate membranes. *Biochim. Biophys. Acta (BBA)—Biomembr.* **1979**, *557*, 9–23. [[CrossRef](#)]
146. Kojima, C.; Hirano, Y.; Yuba, E.; Harada, A.; Kono, K. Preparation and characterization of complexes of liposomes with gold nanoparticles. *Colloids Surf. B Biointerfaces* **2008**, *66*, 246–252. [[CrossRef](#)]
147. Sánchez-López, V.; Fernández-Romero, J.; Gómez-Hens, A. Evaluation of liposome populations using a sucrose density gradient centrifugation approach coupled to a continuous flow system. *Anal. Chim. Acta* **2009**, *645*, 79–85. [[CrossRef](#)]
148. Lee, H.-Y.; Shin, S.H.R.; Abezgauz, L.L.; Lewis, S.A.; Chirsan, A.M.; Danino, D.D.; Bishop, K.J.M. Integration of Gold Nanoparticles into Bilayer Structures via Adaptive Surface Chemistry. *J. Am. Chem. Soc.* **2013**, *135*, 5950–5953. [[CrossRef](#)] [[PubMed](#)]
149. Von White, I.G.; Chen, Y.; Roder-Hanna, J.; Bothun, G.D.; Kitchens, C.L. Structural and Thermal Analysis of Lipid Vesicles Encapsulating Hydrophobic Gold Nanoparticles. *ACS Nano* **2012**, *6*, 4678–4685. [[CrossRef](#)]
150. Nsairat, H.; Khater, D.; Sayed, U.; Odeh, F.; Al Bawab, A.; Alshaer, W. Liposomes: Structure, composition, types, and clinical applications. *Heliyon* **2022**, *8*, e09394. [[CrossRef](#)]
151. De Piano, R.; Caccavo, D.; Lamberti, G.; Remaut, K.; Seynaeve, H.; Barba, A.A. A New Productive Approach and Formulative Optimization for Curcumin Nanoliposomal Delivery Systems. *Pharmaceutics* **2023**, *15*, 959. [[CrossRef](#)]
152. Sudhakar, K.; Fuloria, S.; Subramanian, V.; Sathasivam, K.V.; Azad, A.K.; Swain, S.S.; Sekar, M.; Karupiah, S.; Porwal, O.; Sahoo, A.; et al. Ultraflexible Liposome Nanocargo as a Dermal and Transdermal Drug Delivery System. *Nanomaterials* **2021**, *11*, 2557. [[CrossRef](#)]
153. Sztandera, K.; Gorzkiewicz, M.; Klajnert-Maculewicz, B. Gold Nanoparticles in Cancer Treatment. *Mol. Pharm.* **2019**, *16*, 1–23. [[CrossRef](#)]
154. Sonkar, R.; Sonali, Jha, A.; Viswanadh, M.K.; Burande, A.S.; Narendra; Pawde, D.M.; Patel, K.K.; Singh, M.; Koch, B.; et al. Gold liposomes for brain-targeted drug delivery: Formulation and brain distribution kinetics. *Mater. Sci. Eng. C* **2020**, *120*, 111652. [[CrossRef](#)]
155. Kohout, C.; Santi, C.; Polito, L. Anisotropic Gold Nanoparticles in Biomedical Applications. *Int. J. Mol. Sci.* **2018**, *19*, 3385. [[CrossRef](#)] [[PubMed](#)]
156. Alkilany, A.M.; Nagaria, P.K.; Hexel, C.R.; Shaw, T.J.; Murphy, C.J.; Wyatt, M.D. Cellular Uptake and Cytotoxicity of Gold Nanorods: Molecular Origin of Cytotoxicity and Surface Effects. *Small* **2009**, *5*, 701–708. [[CrossRef](#)] [[PubMed](#)]
157. Alkilany, A.; Shatanawi, A.; Kurtz, T.; Caldwell, R. Toxicity and Cellular Uptake of Gold Nanorods in Vascular Endothelium and Smooth Muscles of Isolated Rat Blood Vessel: Importance of Surface Modification. *Small* **2012**, *8*, 1270–1278. [[CrossRef](#)]
158. Gudlur, S.; Goyal, G.; Pradhan, A.; Ho, J.C.S.; Srivastava, R.; Liedberg, B. Cationic Liposomes Enable Shape Control in Surfactant-Free Synthesis of Biocompatible Gold Nanorods. *Chem. Mater.* **2021**, *33*, 4558–4567. [[CrossRef](#)]
159. Ştiufiuc, G.F.; Niţică, S.; Toma, V.; Iacoviţă, C.; Zahn, D.; Tetean, R.; Burzo, E.; Lucaciu, C.M.; Ştiufiuc, R.I. Synergistical Use of Electrostatic and Hydrophobic Interactions for the Synthesis of a New Class of Multifunctional Nanohybrids: Plasmonic Magneto-Liposomes. *Nanomaterials* **2019**, *9*, 1623. [[CrossRef](#)]

160. Zarchi, A.A.K.; Amini, S.M.; Salimi, A.; Kharazi, S. Synthesis and characterisation of liposomal doxorubicin with loaded gold nanoparticles. *IET Nanobiotechnol.* **2018**, *12*, 846–849. [[CrossRef](#)]
161. Hou, K.; Bao, M.; Xin, C.; Wang, L.; Zhang, H.; Zhao, H.; Wang, Z. Green synthesis of gold nanoparticles coated doxorubicin liposomes using procyanidins for light-controlled drug release. *Adv. Powder Technol.* **2020**, *31*, 3640–3649. [[CrossRef](#)]
162. Zhu, D.; Wang, Z.; Zong, S.; Zhang, Y.; Chen, C.; Zhang, R.; Yun, B.; Cui, Y. Investigating the Intracellular Behaviors of Liposomal Nanohybrids via SERS: Insights into the Influence of Metal Nanoparticles. *Theranostics* **2018**, *8*, 941–954. [[CrossRef](#)]
163. Sugikawa, K.; Kadota, T.; Yasuhara, K.; Ikeda, A. Anisotropic Self-Assembly of Citrate-Coated Gold Nanoparticles on Fluidic Liposomes. *Angew. Chem. Int. Ed.* **2016**, *55*, 4059–4063. [[CrossRef](#)]
164. Kunjiappan, S.; Panneerselvam, T.; Somasundaram, B.; Arunachalam, S.; Sankaranarayanan, M.; Parasuraman, P. Preparation of liposomes encapsulated Epirubicin-gold nanoparticles for Tumor specific delivery and release. *Biomed. Phys. Eng. Express* **2018**, *4*, 045027. [[CrossRef](#)]
165. Alvi, S.B.; Rajalakshmi, P.S.; Jogdand, A.; Sanjay, A.Y.; Veeresh, B.; John, R.; Rengan, A.K. Iontophoresis mediated localized delivery of liposomal gold nanoparticles for photothermal and photodynamic therapy of acne. *Biomater. Sci.* **2021**, *9*, 1421–1430. [[CrossRef](#)]
166. Baxa, U. Imaging of Liposomes by Transmission Electron Microscopy. *Charact. Nanoparticles Intend. Drug Deliv.* **2017**, *1682*, 73–88. [[CrossRef](#)]
167. Sitaula, S.; Mackiewicz, M.R.; Reed, S.M. Gold nanoparticles become stable to cyanide etch when coated with hybrid lipid bilayers. *Chem. Commun.* **2008**, *26*, 3013–3015. [[CrossRef](#)] [[PubMed](#)]
168. Charest, G.; Tippayamontri, T.; Shi, M.; Wehbe, M.; Anantha, M.; Bally, M.; Sanche, L. Concomitant Chemoradiation Therapy with Gold Nanoparticles and Platinum Drugs Co-Encapsulated in Liposomes. *Int. J. Mol. Sci.* **2020**, *21*, 4848. [[CrossRef](#)] [[PubMed](#)]
169. Jhun, J.; Moon, J.; Ryu, J.; Shin, Y.; Lee, S.; Cho, K.-H.; Kang, T.; Cho, M.-L.; Park, S.-H. Liposome/gold hybrid nanoparticle encoded with CoQ10 (LGNP-CoQ10) suppressed rheumatoid arthritis via STAT3/Th17 targeting. *PLoS ONE* **2020**, *15*, e0241080. [[CrossRef](#)]
170. Hachenberger, Y.U.; Rosenkranz, D.; Kriegel, F.L.; Krause, B.; Matschaß, R.; Reichardt, P.; Tentschert, J.; Laux, P.; Jakubowski, N.; Panne, U.; et al. Tackling Complex Analytical Tasks: An ISO/TS-Based Validation Approach for Hydrodynamic Chromatography Single Particle Inductively Coupled Plasma Mass Spectrometry. *Materials* **2020**, *13*, 1447. [[CrossRef](#)]
171. Schulz, M.; Olubummo, A.; Binder, W.H. Beyond the lipid-bilayer: Interaction of polymers and nanoparticles with membranes. *Soft Matter* **2012**, *8*, 4849–4864. [[CrossRef](#)]
172. Le Bihan, O.; Bonnafous, P.; Marak, L.; Bickel, T.; Trépout, S.; Mornet, S.; De Haas, F.; Talbot, H.; Taveau, J.-C.; Lambert, O. Cryo-electron tomography of nanoparticle transmigration into liposome. *J. Struct. Biol.* **2009**, *168*, 419–425. [[CrossRef](#)]
173. Rengan, A.K.; Jagtap, M.; De, A.; Banerjee, R.; Srivastava, R. Multifunctional gold coated thermo-sensitive liposomes for multimodal imaging and photo-thermal therapy of breast cancer cells. *Nanoscale* **2013**, *6*, 916–923. [[CrossRef](#)]
174. Lozano, N.; Al-Jamal, W.T.; Taruttis, A.; Beziere, N.; Burton, N.C.; Bossche, J.V.D.; Mazza, M.; Herzog, E.; Ntziachristos, V.; Kostarelos, K. Liposome–Gold Nanorod Hybrids for High-Resolution Visualization Deep in Tissues. *J. Am. Chem. Soc.* **2012**, *134*, 13256–13258. [[CrossRef](#)] [[PubMed](#)]
175. Appidi, T.; Rajalakshmi, P.S.; Chinchulkar, S.A.; Pradhan, A.; Begum, H.; Shetty, V.; Srivastava, R.; Ganesan, P.; Rengan, A.K. A plasmon-enhanced fluorescent gold coated novel lipo-polymeric hybrid nanosystem: Synthesis, characterization and application for imaging and photothermal therapy of breast cancer. *Nanoscale* **2022**, *14*, 9112–9123. [[CrossRef](#)]
176. Zheng, X.; Liu, Q.; Jing, C.; Li, Y.; Li, D.; Luo, W.; Wen, Y.; He, Y.; Huang, Q.; Long, Y.-T.; et al. Catalytic Gold Nanoparticles for Nanoplasmonic Detection of DNA Hybridization. *Angew. Chem.* **2011**, *123*, 12200–12204. [[CrossRef](#)]
177. Sedighi, A.; Li, P.C.H.; Pekcevik, I.C.; Gates, B.D. A Proposed Mechanism of the Influence of Gold Nanoparticles on DNA Hybridization. *ACS Nano* **2014**, *8*, 6765–6777. [[CrossRef](#)] [[PubMed](#)]
178. Lo, K.-M.; Lai, C.-Y.; Chan, H.-M.; Ma, D.-L.; Li, H.-W. Monitoring of DNA–protein interaction with single gold nanoparticles by localized scattering plasmon resonance spectroscopy. *Methods* **2013**, *64*, 331–337. [[CrossRef](#)]
179. Tsai, C.-S.; Yu, T.-B.; Chen, C.-T. Gold nanoparticle-based competitive colorimetric assay for detection of protein–protein interactions. *Chem. Commun.* **2005**, *34*, 4273–4275. [[CrossRef](#)]
180. Sandhu, K.K.; McIntosh, C.M.; Simard, J.M.; Smith, S.W.; Rotello, V.M. Gold Nanoparticle-Mediated Transfection of Mammalian Cells. *Bioconj. Chem.* **2001**, *13*, 3–6. [[CrossRef](#)]
181. Crew, E.; Rahman, S.; Razzak-Jaffar, A.; Mott, D.; Kamundi, M.; Yu, G.; Tchah, N.; Lee, J.; Bellavia, M.; Zhong, C.-J. MicroRNA Conjugated Gold Nanoparticles and Cell Transfection. *Anal. Chem.* **2011**, *84*, 26–29. [[CrossRef](#)] [[PubMed](#)]
182. Mazur, F.; Tran, H.; Kuchel, R.P.; Chandrawati, R. Rapid Detection of *Listeriolysin O* Toxin Based on a Nanoscale Liposome–Gold Nanoparticle Platform. *ACS Appl. Nano Mater.* **2020**, *3*, 7270–7280. [[CrossRef](#)]
183. Kim, J.; Moon, B.-S.; Hwang, E.; Shaban, S.; Lee, W.; Pyun, D.-G.; Lee, D.H.; Kim, D.-H. Solid-state colorimetric polydiacetylene liposome biosensor sensitized by gold nanoparticles. *Analyst* **2021**, *146*, 1682–1688. [[CrossRef](#)] [[PubMed](#)]
184. Yang, Z.; Malinick, A.S.; Yang, T.; Cheng, W.; Cheng, Q. Gold nanoparticle-coupled liposomes for enhanced plasmonic biosensing. *Sensors Actuators Rep.* **2020**, *2*, 100023. [[CrossRef](#)]
185. Chen, T.; Sheng, A.; Hu, Y.; Mao, D.; Ning, L.; Zhang, J. Modularization of three-dimensional gold nanoparticles/ferrocene/liposome cluster for electrochemical biosensor. *Biosens. Bioelectron.* **2019**, *124–125*, 115–121. [[CrossRef](#)] [[PubMed](#)]

186. Rubio-Camacho, M.; Martínez-Tomé, M.J.; Cuestas-Ayllón, C.; de la Fuente, J.M.; Esquembre, R.; Mateo, C.R. Tailoring the plasmonic properties of gold-liposome nanohybrids as a potential powerful tool for light-mediated therapies. *Colloid Interface Sci. Commun.* **2023**, *52*, 100690. [[CrossRef](#)]
187. Mohammadi, M.; Taghavi, S.; Abnous, K.; Taghdisi, S.M.; Ramezani, M.; Alibolandi, M. Hybrid Vesicular Drug Delivery Systems for Cancer Therapeutics. *Adv. Funct. Mater.* **2018**, *28*, 1802136. [[CrossRef](#)]
188. Pradhan, A.; Kumari, A.; Srivastava, R.; Panda, D. Quercetin Encapsulated Biodegradable Plasmonic Nanoparticles for Photothermal Therapy of Hepatocellular Carcinoma Cells. *ACS Appl. Bio Mater.* **2019**, *2*, 5727–5738. [[CrossRef](#)]
189. Wu, G.; Mikhailovsky, A.; Khant, H.A.; Fu, C.; Chiu, W.; Zasadzinski, J.A. Remotely Triggered Liposome Release by Near-Infrared Light Absorption via Hollow Gold Nanoshells. *J. Am. Chem. Soc.* **2008**, *130*, 8175–8177. [[CrossRef](#)]
190. Agarwal, A.; Mackey, M.A.; El-Sayed, M.A.; Bellamkonda, R.V. Remote Triggered Release of Doxorubicin in Tumors by Synergistic Application of Thermosensitive Liposomes and Gold Nanorods. *ACS Nano* **2011**, *5*, 4919–4926. [[CrossRef](#)]
191. Lajunen, T.; Viitala, L.; Kontturi, L.-S.; Laaksonen, T.; Liang, H.; Vuorimaa-Laukkanen, E.; Viitala, T.; Le Guével, X.; Yliperttula, M.; Murtomäki, L.; et al. Light induced cytosolic drug delivery from liposomes with gold nanoparticles. *J. Control Release* **2015**, *203*, 85–98. [[CrossRef](#)]
192. Zhang, X.; Liu, Y.; Luo, L.; Li, L.; Xing, S.; Yin, T.; Bian, K.; Zhu, R.; Gao, D. A chemo-photothermal synergetic antitumor drug delivery system: Gold nanoshell coated wedelolactone liposome. *Mater. Sci. Eng. C* **2019**, *101*, 505–512. [[CrossRef](#)]
193. Takakura, Y.; Takahashi, Y. Strategies for persistent retention of macromolecules and nanoparticles in the blood circulation. *J. Control Release* **2022**, *350*, 486–493. [[CrossRef](#)]
194. Papini, E.; Tavano, R.; Mancin, F. Opsonins and Dysopsonins of Nanoparticles: Facts, Concepts, and Methodological Guidelines. *Front. Immunol.* **2020**, *11*, 567365. [[CrossRef](#)]
195. Tang, Y.; Wang, X.; Li, J.; Nie, Y.; Liao, G.; Yu, Y.; Li, C. Overcoming the Reticuloendothelial System Barrier to Drug Delivery with a “don’t-Eat-Us” Strategy. *ACS Nano* **2019**, *13*, 13015–13026. [[CrossRef](#)]
196. Zhang, N.; Chen, H.; Liu, A.-Y.; Shen, J.-J.; Shah, V.; Zhang, C.; Hong, J.; Ding, Y. Gold conjugate-based liposomes with hybrid cluster bomb structure for liver cancer therapy. *Biomaterials* **2016**, *74*, 280–291. [[CrossRef](#)]
197. Choi, H.S.; Liu, W.; Misra, P.; Tanaka, E.; Zimmer, J.P.; Ipe, B.I.; Bawendi, M.G.; Frangioni, J.V. Renal clearance of quantum dots. *Nat. Biotechnol.* **2007**, *25*, 1165–1170. [[CrossRef](#)]
198. Al-Jamal, W.T.; Kostarelos, K. Liposomes: From a Clinically Established Drug Delivery System to a Nanoparticle Platform for Theranostic Nanomedicine. *Acc. Chem. Res.* **2011**, *44*, 1094–1104. [[CrossRef](#)]
199. Haraldsson, B.; Nyström, J.; Deen, W.M. Properties of the Glomerular Barrier and Mechanisms of Proteinuria. *Physiol. Rev.* **2008**, *88*, 451–487. [[CrossRef](#)] [[PubMed](#)]
200. Mitchell, M.J.; Billingsley, M.M.; Haley, R.M.; Wechsler, M.E.; Peppas, N.A.; Langer, R. Engineering precision nanoparticles for drug delivery. *Nat. Rev. Drug Discov.* **2020**, *20*, 101–124. [[CrossRef](#)] [[PubMed](#)]
201. García, K.P.; Zarschler, K.; Barbaro, L.; Barreto, J.A.; O’Malley, W.; Spiccia, L.; Stephan, H.; Graham, B. Zwitterionic-Coated “Stealth” Nanoparticles for Biomedical Applications: Recent Advances in Countering Biomolecular Corona Formation and Uptake by the Mononuclear Phagocyte System. *Small* **2014**, *10*, 2516–2529. [[CrossRef](#)]
202. Zalba, S.; Hagen, T.L.T.; Burgui, C.; Garrido, M.J. Stealth nanoparticles in oncology: Facing the PEG dilemma. *J. Control Release* **2022**, *351*, 22–36. [[CrossRef](#)]
203. Nam, J.; Ha, Y.S.; Hwang, S.; Lee, W.; Song, J.; Yoo, J.; Kim, S. pH-responsive gold nanoparticles-in-liposome hybrid nanostructures for enhanced systemic tumor delivery. *Nanoscale* **2013**, *5*, 10175–10178. [[CrossRef](#)] [[PubMed](#)]
204. Bariana, M.; Zhang, B.; Sun, J.; Wang, W.; Wang, J.; Cassella, E.; Myint, F.; Anuncio, S.A.; Ouk, S.; Liou, H.-C.; et al. Targeted Lymphoma Therapy Using a Gold Nanoframework-Based Drug Delivery System. *ACS Appl. Mater. Interfaces* **2023**, *15*, 6312–6325. [[CrossRef](#)] [[PubMed](#)]
205. Morishita, M.; Takahashi, Y.; Nishikawa, M.; Sano, K.; Kato, K.; Yamashita, T.; Imai, T.; Saji, H.; Takakura, Y. Quantitative Analysis of Tissue Distribution of the B16BL6-Derived Exosomes Using a Streptavidin-Lactadherin Fusion Protein and Iodine-125-Labeled Biotin Derivative After Intravenous Injection in Mice. *J. Pharm. Sci.* **2015**, *104*, 705–713. [[CrossRef](#)]
206. Kooijmans, S.A.A.; Fliervoet, L.A.L.; van der Meel, R.; Fens, M.H.A.M.; Heijnen, H.F.G.; van Bergen En Henegouwen, P.M.P.; Vader, P.; Schiffelers, R.M. PEGylated and targeted extracellular vesicles display enhanced cell specificity and circulation time. *J. Control Release* **2016**, *224*, 77–85. [[CrossRef](#)] [[PubMed](#)]
207. Liu, D.; Hu, Q.; Song, Y.K. Liposome clearance from blood: Different animal species have different mechanisms. *Biochim. Biophys. Acta* **1995**, *1240*, 277–284. [[CrossRef](#)]
208. Litzinger, D.C.; Buiting, A.M.; van Rooijen, N.; Huang, L. Effect of liposome size on the circulation time and intraorgan distribution of amphipathic poly(ethylene glycol)-containing liposomes. *Biochim. Biophys. Acta (BBA)—Biomembr.* **1994**, *1190*, 99–107. [[CrossRef](#)]
209. Choi, C.H.J.; Zuckerman, J.E.; Webster, P.; Davis, M.E. Targeting kidney mesangium by nanoparticles of defined size. *Proc. Natl. Acad. Sci. USA* **2011**, *108*, 6656–6661. [[CrossRef](#)]

Disclaimer/Publisher’s Note: The statements, opinions and data contained in all publications are solely those of the individual author(s) and contributor(s) and not of MDPI and/or the editor(s). MDPI and/or the editor(s) disclaim responsibility for any injury to people or property resulting from any ideas, methods, instructions or products referred to in the content.